Sustainable Food Technology

ROYAL SOCIETY OF CHEMISTRY

PAPER

View Article Online
View Journal

Check for updates

Cite this: DOI: 10.1039/d5fb00536a

Improving the recovery of phenolics and flavonoids from *Coriandrum sativum* L. leaves using microwave-enzymatic-assisted extraction

Tan Phat Vo,[ab] Minh Thu Nguyen,[ab] Thuy Anh Nguyen,[ab] Gia Vinh Nguyen,[ab] Hoang Nhan Nguyen,[ab] Gia Bao Pham,[ab] Minh Hoa Ha*[ab] and Dinh Quan Nguyen*[ab]

Received 29th August 2025
Accepted 12th January 2026

DOI: 10.1039/d5fb00536a

rsc.li/susfoodtech

This study focused on optimizing the extraction of phenolic compounds and flavonoids from leaves of *Coriandrum sativum* L. using a sequential green extraction approach based on microwave-enzymatic-assisted extraction (MEAE). Utilizing a glycerol and choline chloride solvent system (composed of Gly–Cho in a molar ratio of 2 : 1, with water), several extraction parameters were systematically investigated to study their influence on total phenolic content (TPC) and total flavonoid content (TFC): solid-to-liquid ratio, water content, microwave power, microwave time, enzyme concentration, and enzyme incubation time. Subsequent optimization established the following conditions: a solid-to-liquid ratio of 1/20 g mL^{-1}, 10% water content in solvent, 1022 W microwave power, 2.6 minutes microwave time, 40 U g^{-1} enzyme concentration, and 90 minutes enzyme incubation time at 50 °C. Under these optimized parameters, the TPC of the extracts reached 18.15 mg GAE g^{-1}, while the TFC reached 26.36 mg RE g^{-1}. The significance of variables was evaluated using the Plackett–Burman design, while optimal conditions were determined *via* the Box–Behnken design. Furthermore, the extraction kinetics were modeled using a second-order kinetic model to understand the mechanism. The findings demonstrate that the sequential MEAE technique, optimized *via* statistical and kinetic models, holds significant promise as an effective green method for enhancing the recovery of antioxidant compounds from *Coriandrum sativum* L.

Open Access Article. Published on 12 janvris 2026. Downloaded on 06.04.2026 16:18:23.
This article is licensed under a Creative Commons Attribution-NonCommercial 3.0 Unported Licence.

Sustainability spotlight

Microwave-enzymatic-assisted extraction is a combination of green technology with great potential in enhancing the extraction yield of bioactive compounds from plants, such as *Coriandrum sativum* L. leaves. Natural deep eutectic solvents are green solvents synthesized by combining organic acid and choline chloride from living organisms' cells. The combination of microwave-enzymatic assisted extraction and natural deep eutectic solvents makes way for the development of sustainable food processing objectives. Microwave-enzymatic-assisted extraction provided rapid heating and hydrolysis of rigid plant cell walls. This combination significantly improves bioactive compounds' extraction yield without deterioration, which usually happens with conventional extraction techniques. Through natural deep eutectic solvents characterization, this work explains how different types of natural deep eutectic solvents affect the recovery yield of bioactive compounds from *Coriandrum sativum* L. leaves. This study also describes the mechanisms of the combined technology based on the support of thermodynamic modeling, scanning electron microscopy, and X-ray diffraction. Results show that careful control of parameters like microwave power and enzyme activity is essential in achieving maximum efficiency without compromising the product quality. This study highlights the technological advantages of Microwave-enzymatic-assisted extraction while supporting its potential for broader adoption as a sustainable, bioactive compound preserving approach in food supply chains. Moreover, it underscores the role of regional biodiversity in driving the development of innovative food products that contribute to human health and environmental sustainability.

1 Introduction

Coriandrum sativum L., known as coriander or cilantro, is a popular cultivated herb in cuisines and traditional medical applications.[1] Native to the Mediterranean and Southwest Asia, it is now extensively grown in regions such as India, China, Egypt, Russia, and other tropical zones. In traditional medicine, coriander supports digestive health and alleviates symptoms including bloating, nausea, and diarrhea. It is also used in the treatment of urinary tract disorders, inflammation, anxiety, and insomnia. Coriander is high in bioactive compounds, especially antioxidants.[2] Significant amounts of flavonoids, carotenoids, and phenolic compounds – in particular, gallic acid, ferulic acid – have been found through quantitative analyses. These phenolics possess antioxidant capacity by scavenging free radicals, which is a significant contributor to the development of chronic diseases such as diabetes, cancer, heart disease, and neurological

[a]Laboratory of Biofuel and Biomass Research, Faculty of Chemical Engineering, Ho Chi Minh City University of Technology (HCMUT), 268 Ly Thuong Kiet Street, District 10, Ho Chi Minh City, Vietnam. E-mail: ndquan@hcmut.edu.vn; hoa.ha169@hcmut.edu.vn
[b]Vietnam National University Ho Chi Minh City, Linh Trung Ward, Thu Duc City, Ho Chi Minh City, Vietnam

© 2026 The Author(s). Published by the Royal Society of Chemistry

Open Access Article. Published on 12 janvris 2026. Downloaded on 06.04.2026 16:18:23.
This article is licensed under a Creative Commons Attribution-NonCommercial 3.0 Unported Licence.

disorders. Additionally, these drugs support cardiovascular health by reducing blood pressure and low-density lipoprotein cholesterol. Iram Iqbal *et al.* (2023) stated that plant polyphenols can prevent atherosclerosis by regulating vascular endothelial function through the release of nitric oxide (NO) and reducing LDL oxidation to prevent atherosclerosis. Cardiovascular diseases, such as stroke, hypertension, and ischemic heart disease, can be prevented by dietary polyphenols.[3]

Extracting phenolic compounds from *Coriandrum sativum* L. is necessary to obtain beneficial active components, and the selection of solvent greatly influences the effectiveness of this process. Traditional solvents, such as methanol, ethanol, and acetone, are gradually being replaced by more environmentally friendly alternatives in the pursuit of sustainable and eco-friendly solutions. Natural Deep Eutectic Solvents (NDESs) represent one such promising alternative. NDESs are an emerging class of solvents, typically formed from mixtures of two or more pure solid or liquid components.[4] When mixed in specific proportions, these components form a mixture with a melting point that is significantly lower than that of each pure component.

This low melting point is typically below room temperature, rendering the mixture a liquid at room temperature. NDESs are distinguished by several excellent properties, making them an attractive choice for extracting natural compounds. One of the most important is their low melting point, which allows them to exist in a liquid state without needing much energy. In addition, NDESs are highly regarded for their safety due to their low toxicity, non-volatility, and non-flammability, making them more environmentally and user-friendly than traditional organic solvents. The recyclability and reusability of many NDESs help reduce waste and costs. Finally, the tunable properties allow scientists to change the composition to optimize solubility for each specific target compound. NDESs are opening a new era of sustainable and efficient extraction methods.[4]

Traditional extraction procedures, such as maceration, Soxhlet extraction, and reflux, are inexpensive and straightforward; however, they can be time-consuming, solvent-intensive, and inefficient. Furthermore, prolonged exposure to heat during these operations can damage sensitive substances. To address these drawbacks, advanced extraction technologies have been developed to improve efficiency, reduce processing time and solvent use, and better preserve the bioactivity of target compounds.[5] Among these, Microwave-Assisted Extraction (MASE) and Enzyme-Assisted Extraction (EASE) are two prominent techniques. MASE utilizes microwave energy to rapidly heat and pressurize plant cells, causing them to rupture and release phenolic compounds.[6] EASE uses hydrolytic enzymes such as cellulases, hemicellulases, and pectinases to break down the plant cell wall matrix and release intracellular phenolics into the solvent. While both MASE and EASE provide considerable advantages over traditional approaches, combining the two has emerged as a promising strategy. Microwaves are first used in this combined method to break down the structures and speed up the diffusion of phenolic compounds into the NDES. The enzyme is then used to further weaken or break down the cell wall.

A comparative study demonstrated MASE's effectiveness in isolating quercetin 3-*O*-glucoside, a bioactive compound with anti-diabetic properties, from *Gynura procumbens*.[6] The MASE method demonstrated significant advantages over conventional Soxhlet extraction, requiring only 5 minutes of extraction time compared to 3 hours and yielding a higher amount of quercetin (1.60 mg g^{-1} *vs.* 1.40 mg g^{-1}). A custom-designed temperature-controlled MASE system was developed to enhance extraction efficiency and prevent the thermal degradation of bioactive compounds. This system utilizes feedback from a temperature sensor to regulate microwave output, ensuring precise thermal control throughout the process. These findings confirm that MASE, particularly in terms of temperature regulation, is a highly efficient and viable technique for extracting thermally sensitive bioactive compounds.[6] A food-friendly enzyme-assisted extraction (EASE) method was developed and refined by Mridusmita Chaliha *et al.* to extract bioactive substances from freeze-dried Kakadu plum puree. To optimize the yields of free ellagic acid (fEA), ascorbic acid, and phenolics, they ascertained the ideal parameters for solvent concentration, enzyme concentration, and extraction duration. With a yield of 51.3%, the study found that the best conditions for extracting fEA were 1.5% (w/w) propylene glycol, 300 mg L^{-1} pectolytic enzyme, and a 15 hour extraction period.[7] While previous studies have applied either MASE or EASE individually, few have systematically optimized their integration or identified the factors influencing extraction efficiency. The kinetic behavior and underlying mechanisms of the combined process also remain insufficiently elucidated.[8]

Therefore, this study focuses on optimizing the integrated MASE–EASE process using NDESs to enhance the extraction efficiency and improve the recovery of bioactive compounds from *Coriandrum sativum* L. leaves. Various extraction parameters, including solid-to-liquid ratio, water content, microwave power, enzyme concentration, and incubation time, were systematically optimized using the Plackett–Burman and Box–Behnken designs. The extraction kinetics were modeled using a second-order kinetic model to elucidate the mass transfer mechanism. Additionally, the reusability of the NDES and the cost and energy efficiency of the optimized MEAE process were evaluated to assess its industrial feasibility.

2 Materials and methods

2.1 Materials

We purchased *Coriandrum sativum* from Binh Dien Wholesale Market in Ho Chi Minh City, Vietnam (the producing region is the Mekong Delta). To enable water evaporation, the samples were kept in a laboratory dryer (model: TR-240, Nabertherm, Zürich, Germany) for 48 hours at 50 °C. A dried coriander powder (DCP) was obtained by grinding dried leaves in a grinder (model: SM 450L, Harlow, UK). The final powder was kept in an airtight plastic container and stored at 25 °C in a dry place, without direct sunlight. These storage conditions were chosen to maintain the stability of the bioactive compounds while also preventing moisture absorption and inhibiting microbial growth.

© 2026 The Author(s). Published by the Royal Society of Chemistry

Open Access Article. Published on 12 janvris 2026. Downloaded on 06.04.2026 16:18:23.
This article is licensed under a Creative Commons Attribution-NonCommercial 3.0 Unported Licence.

Table 1 Details of 15 synthesized NDESs[a]

No.	Solvent	HBD	HBA	pH	Density (g mL^{-1})
NDES1	Lac–Cho	Lactic acid	Choline chloride	0.97	1.156 ± 0.015h
NDES2	Lac–Gly	Lactic acid	Glycerol	0.60	1.186 ± 0.023fg
NDES3	Lac–Pro	Lactic acid	1,2-Propanediol	1.10	1.116 ± 0.014i
NDES4	Lac–Ery	Lactic acid	Erythritol	0.91	1.274 ± 0.006d
NDES5	Ci–Cho	Citric acid	Choline chloride	−0.52	1.384 ± 0.009c
NDES6	Ci–Gly	Citric acid	Glycerol	−0.72	1.414 ± 0.011b
NDES7	Ci–Pro	Citric acid	1,2-Propanediol	−1.67	1.444 ± 0.007a
NDES8	Ci–Ery	Citric acid	Erythritol	−1.59	1.434 ± 0.015ab
NDES9	Gly–Cho	Glycerol	Choline chloride	3.36	1.164 ± 0.008gh
NDES10	Pro–Cho	1,2–Propanediol	Choline chloride	3.14	1.234 ± 0.006e
NDES11	Ace–Cho	Acetic acid	Choline chloride	0.02	1.092 ± 0.015j
NDES12	Ace–Ery	Acetic acid	Erythritol	0.18	1.114 ± 0.020ij
NDES13	Ace–Gly	Acetic acid	Glycerol	−0.14	1.052 ± 0.008k
NDES14	Ace–Pro	Acetic acid	1,2-Propanediol	−0.84	1.032 ± 0.017k
NDES15	Ery–Cho	Erythritol	Choline chloride	2.47	1.206 ± 0.014f

[a] The letters a, b… and k represent statistically significant differences. Samples sharing the same letters (*e.g.*, fg and gh or a and ab) are not significantly different in density, while samples with different letters are significantly different.

2.2 Chemicals

Chemicals used to prepare NDESs included glycerol (Duc Giang Chemicals Group Jsc, Hanoi, Vietnam); acetic acid, lactic acid, and citric acid (Guangdong Guanghua Sci-Tech Co., Ltd, Guangdong, China); choline chloride (HiMedia Laboratories Pvt. Ltd, Nasik, India); and erythritol and 1,2-propanediol (Hoa Nam Chemicals – Laboratory Equipment Company, Ltd).

The following analytical reagents were used: aluminum chloride ($AlCl_3$), sodium carbonate (Na_2CO_3), sodium acetate (CH_3COONa), ethanol (96%), and the Folin–Ciocalteu phenol reagent. Hoa Nam Chemicals – Laboratory Equipment Company, Ltd (Ho Chi Minh City, Vietnam) was the supplier of all chemicals.

2.3 Preparation for NDESs

To assess their phenolic and flavonoid extractability from DCP, fifteen distinct NDESs were chosen, each with the same formulation and abbreviation shown in Table 1. A 2 : 1 molar ratio was applied to combine hydrogen bond donors (HBDs) and acceptors (HBAs). Then, a magnetic stirrer (model MS-H380-Pro, DLAB Scientific Co. Ltd, USA) was used to stir and heat the mixture to 80 °C until it became transparent and homogeneous. The solvents were acceptable for synthesis when they did not crystallize at room temperature.

The functional groups in NDESs were analyzed using the Fourier Transform Infrared method, following the previous study.[9] A drop of each NDES was pipetted into the sample holder of the PerkinElmer Spectrum 10.5.2 instrument (Model Frontier FT-IR/NIR 105667, USA), and the spectrum was recorded within the 450–4000 cm^{-1} range. The pH values of the NDESs were measured using a pH meter (Model MI-151, Milwaukee, Romania, EU), while their densities were determined through mass and volume measurements.

2.4 Single-factor experiments of microwave-assisted and enzyme-assisted extraction

In an amber glass vial, 10 mL of solvent was mixed with a precisely measured amount of DCP. Microwave radiation was applied to the mixture (model MOB-7733, TA RA Joint Stock Company, Vietnam). The experiment encompassed solid-to-liquid ratios (SLRs) of 1/10, 1/20, 1/30, 1/40, 1/50, and 1/60 g mL^{-1}, water content (WC) ranging from 0% to 50%, and specific microwave power (MP) settings of 0, 150, 300, 450, 600, 750 and 900 W applied for various microwave times (MTs) of 0.5, 1, 2, 3, and 4 minutes. Following microwave treatment, the samples were cooled to 50 °C. Different enzyme (EC) concentrations, ranging from 0 to 50 U g^{-1}, were added at 10 U intervals. A water bath (Model RS22L, 40 kHz, Rama Vietnam Joint Stock Company, Vietnam) was used for the enzymatic incubation at a temperature (EITem) of 50 °C for enzyme incubation times (EITs) of 30, 60, 90, 120, and 150 minutes. After incubation, the blend was filtered through filter paper to extract the bioactive compounds. The single-factor experiments are shown in Table S1.

2.5 Quantification of bioactive compound recovery

2.5.1 Total phenolic content (TPC). TPC was measured using the spectrophotometry method with minor changes.[10] 0.25 mL of diluted DCP sample was added to a test tube, followed by 0.25 mL of 10% (v/v) Folin & Ciocalteu's reagent (0.19 N). After that, the sample was incubated in the dark for 5 minutes before adding 0.5 mL of 7.5% (w/v) sodium carbonate (Na_2CO_3) and 4 mL of distilled water. The solution was left to react for 1 hour in a dark place at room temperature. The sample absorbance was measured using a UV-visible spectrophotometer (model: Cary 60, Agilent Technologies, USA) at an absorbance wavelength of 765 nm. TPC was expressed as milligrams of gallic acid equivalent per gram (mg GAE g^{-1}).

2.5.2 Total flavonoid content (TFC). TFC was measured with minor changes using the spectrophotometry technique.[11]

Open Access Article. Published on 12 janvris 2026. Downloaded on 06.04.2026 16:18:23.
This article is licensed under a Creative Commons Attribution-NonCommercial 3.0 Unported Licence.

0.50 mL of diluted DCP sample was dispersed in 1.00 mL of 96° ethanol. Then, 0.10 mL of 1 M potassium acetate (CH_3COOK) solution, 0.10 mL of 10% aluminum trichloride solution ($AlCl_3$), and 3.5 mL of distilled water were added. The mixtures were left in a dark room for half an hour. Using an absorbance wavelength of 415 nm, the sample absorbance was measured with a UV-visible spectrophotometer (model: Cary 60, Agilent Technologies, USA). Milligrams of rutin equivalent per gram (mg RE g^{-1}) was the unit of measurement used to express TFC.

2.6 Design of experiments

2.6.1 Plackett–Burman design (PBD) model. In this study, PBD was utilized to identify critical elements that significantly impact the extraction yields of DCP. PBD was selected for this study due to its efficiency in screening multiple variables with minimal experimental runs, requiring only 12 trials to assess six factors for each compound under investigation. Given that PBD focuses on main effects without considering interactions between factors, it is particularly suitable for estimating the individual contributions of each factor in the process, making it a valuable tool for preliminary screenings.[12] TPC and TFC were assessed as dependent responses, using "−1" and "+1" for the six tested components: solid-to-liquid ratio (SLR), water content (WC), microwave power (MP), microwave time (MT), enzyme concentration (EC), and enzyme incubation time (EIT). With this standard, the baseline condition was set at "0", with "−1" denoting the lower level and "+1" the higher level. Eqn (1) shows the relationship between the independent and dependent variables in the experiments.

$$y = \sum_{i=1}^{n} \beta_i x_i \tag{1}$$

where x is the independent variable, y is the response variable, β is the regression coefficient, and i is the order of factors that were examined and how they affected the yield of each targeted compound; x_1, x_2, x_3, x_4, x_5, and x_6 are SLR, WC, MP, MT, EC, and EIT, respectively; y_1 and y_2 are phenolics and flavonoids, respectively; n is the number of factors examined ($n = 6$). In the DCP extraction procedure, parameters with a p-value less than 0.05 significantly affected the yield of flavonoids and phenolics. The details of PBD are shown in Table S2.

2.6.2 Box–Behnken design (BBD) model. The BBD enhanced the extraction process further once the PBD data were analyzed. Fourteen experimental runs, including two center points, were conducted to evaluate the connection between the response variables and specific independent variables. Eqn (2) describes how the data were fitted to a second-order polynomial model:

$$y = \beta_0 + \sum_{i=0}^{n} \beta_0 \beta_i + \sum_{i=0}^{n} \beta_{ii} {\beta_i}^2 + \sum_{i=0}^{n} \sum_{j=0}^{n} \beta_{ij} \beta_i \beta_j \tag{2}$$

where y is the predicted response, β_0 represents the intercept, and β_i, β_{ii}, and β_{ij} are the coefficients for linear, quadratic, and interaction terms, respectively. In this study, the dependent responses are defined as y_1 for TFC expressed in (mg RE g^{-1}) and y_2 for TPC expressed in (mg GAE g^{-1}). The prediction error (%) between the experimental and predicted values was calculated according to eqn (3) to assess the model's accuracy:

$$\text{prediction error} = \frac{\text{The mean of measured value-predicted value}}{\text{The mean of measured value}} \times 100 \tag{3}$$

2.7 Second-order extraction kinetic models

Second-order models were used to investigate the extraction kinetics of MEAE for recovering terpenoids and flavonoids from DCP. These models, which are based on the Ho & McKay model,[13] explain how quickly certain chemicals dissolve in solvents from powder (eqn (4)):

$$\frac{dC_t}{dt} = k\ (C_s - C_t)^2 \tag{4}$$

In the kinetic model, C_s denotes the equilibrium concentration of flavonoids or phenolic compounds (mg g^{-1}), while C_t represents their concentration at a given extraction time t (mg g^{-1}). The parameter k indicates the second-order extraction rate constant (g mg^{-1} min^{-1}), whereas t represents the extraction duration in minutes.

A linear eqn (5) is obtained by solving the differential eqn (4) and rearranging:

$$\frac{t}{C_t} = \frac{t}{C_s} + \frac{1}{kC_s^2} \quad \text{or} \quad y = at + b \tag{5}$$

In this linear form, y corresponds to $\frac{t}{C_t}$; a corresponds to $\frac{1}{C_s}$; b corresponds to $\frac{1}{kC_s^2}$

When the extraction time t is zero, the initial extraction rate, h (mg min^{-1} g^{-1}), is given by eqn (6):

$$h = kC_s^2 \tag{6}$$

Using eqn (5), the second-order extraction rate constant (k) is calculated by plotting $\frac{t}{C_t}$ *versus* t. Eqn (7) is used to determine the Arrhenius constant (E_a, g mg^{-1} min^{-1}) and the activation energy (E_a, kJ mol^{-1}):

$$\ln k = \ln A_e - \frac{A_e}{RT} \tag{7}$$

2.8 NDES recycle procedure

The reusability of NDES9 was evaluated using AB-8 macroporous resin as an adsorbent, as described in a previous study.[14] Before use, the AB-8 resin was immersed in absolute ethanol for 24 hours, and the AB-8 macroporous resin was thoroughly rinsed with ultrapure water to remove residual ethanol. It was stored in water until further use. First, NDES and DCP were mixed and then the MEAE process was performed under optimized conditions. NDES extracts were passed through a glass chromatography column (20 cm bed height) packed with AB-8 resin at a flow rate of 1.0 bed volume (BV)·h^{-1} at 25 °C. This allowed selective adsorption of phenolics and flavonoids onto the resin, while the NDES was recovered in the effluent (NDES-

© 2026 The Author(s). Published by the Royal Society of Chemistry

Open Access Article. Published on 12 janvris 2026. Downloaded on 06.04.2026 16:18:23.
This article is licensed under a Creative Commons Attribution-NonCommercial 3.0 Unported Licence.

reused). After adsorption, the column was first eluted with 70° ethanol to desorb phenolic/flavonoid compounds.[14] NDES-reused was collected and reused directly in subsequent extraction cycles under the same MEAE conditions. The extraction efficiency (%) was determined as the ratio of the TPC and TFC yields obtained in each reuse cycle to those from the fresh solvent. The reusability of the NDES was evaluated through 5 cycles.[15]

2.9 Cost and energy estimation

The economic and energy requirements of the optimized MEAE process were estimated on a 1 L batch basis. The total operating cost (C_{total}) was calculated as the sum of the energy consumption and solvent cost:

$$C_{total} = C_{energy} + C_{solvent}$$

The total energy demand (E_{total}) consisted of three main components, which are microwave heating, enzymatic incubation, and solvent evaporation.

$$E_{total} = E_{microwave} + E_{incubation} + E_{evaporation}$$

Each term was calculated using:

$$E = P \times t$$

where P is the power rating of the equipment (kW) and t is the operation time (hour).

The energy required to heat or evaporate the solvent was additionally estimated using

$$Q = m \times C_p \times \Delta T$$

and

$$Q_{evaporation} = m \times L_v$$

where m is the solvent mass (kg), C_p is the specific heat capacity (kJ kg^{-1} K^{-1}), ΔT is the temperature difference (K), and L_v is the latent heat of vaporization (kJ kg^{-1}).

The energy cost was then determined as

$$C_{energy} = E_{total} \times \text{electricity price}$$

The solvent cost was calculated from the mass of each chemical component in the NDES formulation

$$C_{solvent} = \sum m_i \times p_i$$

where m_i is the mass (kg) and p_i is the market price (USD kg^{-1}) of component i.

The total operating cost per batch and cost per unit of extracted phenolic yield were compared between NDES-based and water-based extraction systems to evaluate process efficiency and scalability.

2.10 Antioxidant activity determination

Antioxidant activities were measured using a UV-visible spectrophotometer and a colorimetric method. Trolox was used as a reference to create standard calibration curves (0–40 mg TAE g^{-1}) to determine the results.

2.10.1 ABTS. Following a previously reported protocol, the ABTS radical scavenging experiment measured absorbance at 734 nm using a UV-visible spectrophotometer.[16] To make the $ABTS^+$ radical solution, 7.40 mM ABTS and 2.45 mM potassium persulfate were fully mixed in a 1 : 1 volume ratio and incubated for 18 hours at 25 °C in the dark. To assess the antioxidant activity, 3.90 mL of the resulting $ABTS^+$ solution and 0.10 mL of the diluted crude sample extract (CSE) were combined. After a 20 minute dark incubation, spectrophotometric analysis was performed. To express the results, the unit of measurement was Trolox equivalents per gram (μM TAE g^{-1}).

2.10.2 DPPH. A UV-visible spectrophotometer set to a detection wavelength of 515 nm was used to perform the DPPH radical scavenging experiment following a previously documented protocol.[17] In this experiment, 3.50 mL of ethanolic DPPH solution was mixed with 0.50 mL of the diluted crude sample extract (CSE). The mixture was then exposed to spectrophotometric analysis after being in the dark for 30 minutes. To express the results, the unit of measurement was Trolox equivalents per gram (μM TAE g^{-1}).

2.10.3 Hydroxyl radical. Using a previously published technique, the hydroxyl radical (˙OH) scavenging activity was assessed by measuring absorbance at 510 nm using UV-visible spectrophotometry.[18] Three stock solutions—8.8 mM hydrogen peroxide, 6 mM salicylic acid, and 9 mM ferrous sulfate ($FeSO_4$)—were prepared for the assay and mixed in a 2 : 5 : 5 volume ratio to create the reaction mixture. 2.4 mL of the reaction mixture and 1.6 mL of the diluted CSE were combined for analysis, which was then spectrophotometrically examined after incubation in the dark for 15 minutes. The findings were presented as mg TAE g^{-1}, or μM Trolox equivalents per gram.

2.10.4 FRAP. A UV-visible spectrophotometer was used to quantify absorbance at 593 nm during the FRAP assay, which was carried out following a previously defined procedure.[19] An acetate buffer (pH 3.6), 20 mM ferric chloride ($FeCl_3$), and a FRAP solution diluted in 10 mM hydrochloric acid were combined in a volumetric ratio of 10 : 1 : 1 to create the working reagent. Before spectrophotometric examination, 0.1 mL of the diluted CSE was combined with 3.9 mL of the newly made working reagent, and the mixture was incubated for 20 minutes. The findings were presented as mg TAE g^{-1}, or μM Trolox equivalents per gram.

2.11 Scanning electron microscopy (SEM) and X-ray diffraction (XRD) of DCP. The surface morphology of DCP following various extraction methods – including CE, MASE, EASE, and MEAE – was characterized using scanning electron microscopy (SEM). Prior to analysis, the extracted residues were dried at 85 °C for 24 hours in an oven until a constant weight was reached. The dried samples were mounted on carbon tape affixed to SEM sample stubs and examined using a gaseous

Open Access Article. Published on 12 janvris 2026. Downloaded on 06.04.2026 16:18:23.
This article is licensed under a Creative Commons Attribution-NonCommercial 3.0 Unported Licence.

secondary electron detector operating in SEM mode to assess changes in surface structure and morphological features.[16]

To evaluate the crystallinity of DCP, both untreated and treated samples were analyzed using X-ray diffraction (XRD). Measurements were performed with a D/max-RAX diffractometer (D8 Advance, Bruker, Germany). The cellulose crystallinity index (CCI) was subsequently calculated using eqn (8), allowing for quantitative comparison of structural modifications resulting from the different extraction treatments.[20]

$$\mathrm{CCI} = \frac{I_{\mathrm{cry}} - I_{\mathrm{amp}}}{I_{\mathrm{cry}}} \times 100\% \quad (8)$$

I_{cry} and I_{amp} are the intensity of the crystalline areas at θ22.5 and the amorphous intensity at θ18.

2.12 Statistical analysis

To ensure reproducibility, all experimental procedures were carried out in triplicate. The mean values and their accompanying standard deviations were used to express the results. OriginPro software (2022 version, OriginLab) was used to visualize data for individual variables, and Design Expert (version 13, Stat-Ease Inc., USA) was used to generate three-dimensional response surface graphs showing how experimental elements interacted. Minitab software (version 19.1) was used to perform statistical analyses, including analysis of variance (ANOVA), using a 95% confidence level ($\alpha = 0.05$) for statistical significance.

3 Results and discussion

3.1 Properties of solvents

3.1.1 FTIR. The functional groups and hydrogen bonding interactions found in several NDESs were examined using FTIR spectroscopy; the corresponding spectra are shown in Fig. 1. Hydrogen bonds between the hydroxyl groups of polyols and carboxylic acids are indicated by a large O–H stretching vibration band seen between 3060 cm^{-1} and 3700 cm^{-1}.[21] Additionally, N–H stretching bands detected in the range of 3447–3349 cm^{-1} suggest hydrogen bonding interactions between the tertiary ammonium groups of choline chloride and carboxylic acids. A characteristic peak around 1709–1730 cm^{-1} was attributed to the C=O stretching vibrations of carboxylic acids such as lactic acid, citric acid, and acetic acid. Peaks near 1645 cm^{-1} across all samples corresponded to C=C stretching vibrations.[22] Bands in the 1195–1397 cm^{-1} range provided additional proof of hydrogen bonding between the C=O group of carboxylic acids and the tertiary ammonium group of choline chloride. Similar vibrations were detected in choline chloride-based systems at 1480 cm^{-1} and 1415 cm^{-1}, whereas peaks at 1458 cm^{-1} and 1376 cm^{-1} were linked to $-CH_3$ bending and –CH bending vibrations, respectively, for lactic acid-based NDESs. The stretching and bending vibrations of the C–H, C–C, C–O, and OCO groups were associated with broader absorption bands in the 1195–953 cm^{-1} area, suggesting structural complexity in the NDES matrices.[23] These spectral

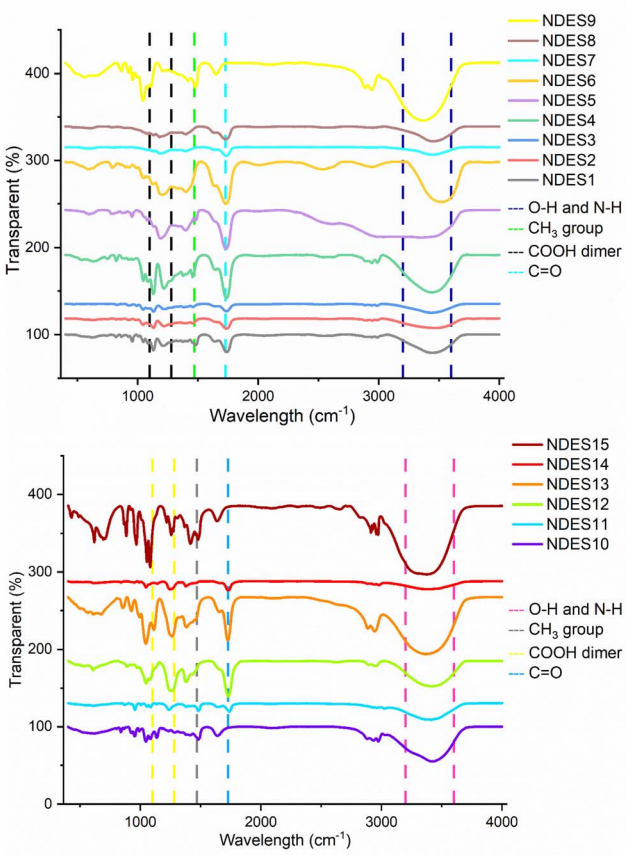

Fig. 1 FTIR spectra of NDESs.

features align with previous studies on choline chloride-based NDESs, such as those involving *Castanea mollissima*,[24] thereby confirming the successful formation of NDESs through hydrogen bonding between carboxylic acids and both polyols and choline chloride.

3.1.2 Density. One of the primary physicochemical characteristics of NDESs is their density, which directly impacts the effectiveness of extraction and separation procedures. As seen in Table 1, the densities of various NDESs vary considerably, ranging from 1.032 g mL^{-1} (Ace-Pro) to 1.444 g mL^{-1} (Ci-Pro), suggesting that their composition and intermolecular interactions are important factors. All tested NDESs exhibited densities greater than 1 g mL^{-1}, which is considerably higher than those of common organic solvents, such as ethanol and hexane.

The density of NDESs reflects the structural differences and the extent of interaction between their HBD and HBA components.[25] Density indicates the strength of the hydrogen bond network formed within the NDES, which in turn influences the solvent's stability and its ability to dissolve target compounds. Among the tested solvents, a citric acid-based NDES (Ci-Pro) exhibited the highest density of 1.444 g mL^{-1}. This trend can be attributed to citric acid's multiple hydroxyl and carboxyl groups, which facilitate the development of a vast network of hydrogen bonds. In contrast, an acetic acid-based NDES (Ace-Pro) showed the lowest density at 1.032 g mL^{-1}, likely due to its shorter carbon chain and fewer functional groups for hydrogen bonding. This trend aligns with previous findings that

© 2026 The Author(s). Published by the Royal Society of Chemistry

Open Access Article. Published on 12 janvris 2026. Downloaded on 06.04.2026 16:18:23.
This article is licensed under a Creative Commons Attribution-NonCommercial 3.0 Unported Licence.

NDESs formed with longer-chain or more hydroxylated organic acids tend to have higher densities. Additionally, NDESs based on organic acids generally have higher densities than those based on polyols, as sugar-derived components, despite being denser in their pure form, tend to form less compact hydrogen-bonding networks in NDES mixtures.[26]

3.1.3 pH. The pH value of NDESs plays a critical role, influencing their chemical reactivity, solution stability, and biological safety. As shown in Table 1, the pH values of NDESs range from −1.67 (Ci-Pro) to 3.36 (Gly-Cho), reflecting the varying acid–base characteristics of their constituent components. Since pH is the negative logarithm to the base 10 of H^+ concentration, values greater than 1 mol L^{-1} result in a negative pH. Among the NDESs formulated with organic acids as HBDs, those based on citric acid (*e.g.*, Ci-Pro and Ci-Ery) exhibit the lowest pH values. This trend aligns with the fact that citric acid has a low first pK_a (∼3.1), indicating a strong tendency to release protons (H^+), thereby creating a more acidic medium.[27] Furthermore, the multiple carboxyl and hydroxyl groups on citric acid facilitate the formation of a dense hydrogen bonding network, which stabilizes the system and maintains a consistently low pH level. Although acetic acid has a higher pK_a than lactic acid, the NDESs prepared with acetic acid (*e.g.*, Ace-Pro) display higher pH values than those made with citric acid. This can be attributed to the weaker hydrogen bonding interactions in acetic-based NDESs, which result in a lower capacity to stabilize and retain free H^+ ions in the solution. Consequently, this leads to a relatively higher pH compared to citric-based systems.

3.1.4 Effect of NDES types. A total of fifteen NDESs were prepared by combining HBDs (lactic acid, citric acid, and acetic acid) with hydrogen bond acceptors HBAs (glycerol, choline chloride, erythritol, and 1,2-propanediol). Notably, glycerol, erythritol, and 1,2-propanediol functioned as both HBAs and HBDs. The extraction performance of these NDESs was assessed under standardized conditions: a SLR of 1 : 20 g mL^{-1}, a WC of 20% (w/w), and a MP of 728 W for 2 minutes, followed by enzymatic treatment with 30 U g^{-1} of EC and incubation at 50 °C for 90 minutes. Fig. 2A presents the TPC and TFC extracted from *Coriandrum sativum* using the fifteen NDES formulations. The results revealed that Gly-Cho (NDES9) exhibited the highest extraction performance, yielding 11.31 ± 0.27 mg GAE g^{-1} of total phenolics and 16.92 ± 1.10 mg RE g^{-1} of total flavonoids. Conversely, Ci-Ery (NDES8) showed the lowest TPC recovery (3.23 ± 1.05 mg GAE g^{-1}), while Ci-Cho (NDES5) produced the lowest TFC yield (1.09 ± 0.16 mg RE g^{-1}).

The extraction efficiency of a NDES is strongly influenced by solvent polarity, which determines the solubility and interaction between the solvent and target compounds. When the polarity of the solvent is compatible with that of the solute, it enhances solubility, promotes efficient mass transfer, and consequently results in higher extraction yields.[28] The partition coefficient (log *P*) serves as an indicator of molecular polarity, where smaller log *P* values reflect greater polarity of compounds or solvents. Among the HBDs, glycerol demonstrates a notably low log *P* of −1.76,[29] signifying its high polarity. Likewise, the HBA choline chloride exhibits pronounced ionic and polar characteristics, allowing for strong interactions with hydrophilic solutes, such as phenolic compounds. Beyond polarity, the physicochemical characteristics of NDESs play a crucial role in determining their efficiency in recovering bioactive compounds. Excessive acidity in solvents can promote degradation or ionization of sensitive molecules, consequently lowering extraction efficiency.[30] In this study, NDES9 (pH = 3.36) provided an optimal medium for the stabilization and solubilization of phenolic compounds. In contrast, highly acidic solvents such as NDES8 (pH = −1.59) and NDES5 (pH = −0.52) may compromise the structural integrity of polyphenols, resulting in reduced recovery. Additionally, solvent density affects both phase dispersion and mass transfer behavior; higher densities, as observed in NDES8 (1.434 g mL^{-1}) and NDES5 (1.384 g mL^{-1}), can restrict solvent penetration into the plant matrix. With a moderate density of 1.164 g mL^{-1}, NDES9 achieved a better balance between diffusivity and interaction with the solid phase.[31] Therefore, NDES9 was chosen as the extraction medium for the recovery of phenolics and flavonoids in subsequent experiments.

3.2 Single-factor experiments

3.2.1 Impact of solid-to-liquid ratio. The effects of the SLR on the extraction of TFC and TPC are illustrated in Fig. 2B. The experiments were performed using NDES9 with six different SLR levels: 1/10, 1/20, 1/30, 1/40, 1/50, and 1/60 g mL^{-1}. As the SLR increased from 1/10 to 1/20 g mL^{-1}, the yields of both TPC and TFC rose significantly. In the study by Wong *et al.* (2013) on *Phyllanthus niruri*, increasing the solvent-to-solid ratio from 10 : 1 to 14 : 1 significantly improved phenolic extraction and antioxidant activity. This enhancement is based on a strong concentration gradient between the solid phase and the solvent, which increases mass transfer. Therefore, the driving force for diffusion increased, facilitating the release of phenolic compounds into the solvent and improving extraction efficiency.[32] Beyond the peak point, both TPC and TFC yields gradually declined. The observed decrease can be ascribed to an excessive amount of solvent, which lowers microwave energy absorption per unit mass of solid. This leads to a reduction in energy density, thereby weakening the thermal effects for extraction. As a result, the disruption of plant cellular structures to release bioactive compounds is limited.[33] Overall, an SLR of 1/20 g mL^{-1} was identified as the most favorable condition for maximizing the recovery of both TPC and TFC from coriander using the MEAE process.

3.2.2 Impact of water content. The effects of WC in NDES9 on the extraction of TFC and TPC are illustrated in Fig. 2C. In this experiment, water was added to the extraction solvent at 0%, 10%, 20%, 30%, 40%, and 50%. As WC increased from 0% to 20%, TPC and TFC content extraction increased significantly. Since water has a high dielectric constant and can efficiently absorb microwave energy, this improvement can be attributed to the better dielectric characteristics of the water–solvent mixture. Therefore, higher WC promotes matrix swelling and enhances the heating efficiency, releasing more phenolic and flavonoid compounds.[17] However, when the water content

Open Access Article. Published on 12 janvris 2026. Downloaded on 06.04.2026 16:18:23.
This article is licensed under a Creative Commons Attribution-NonCommercial 3.0 Unported Licence.

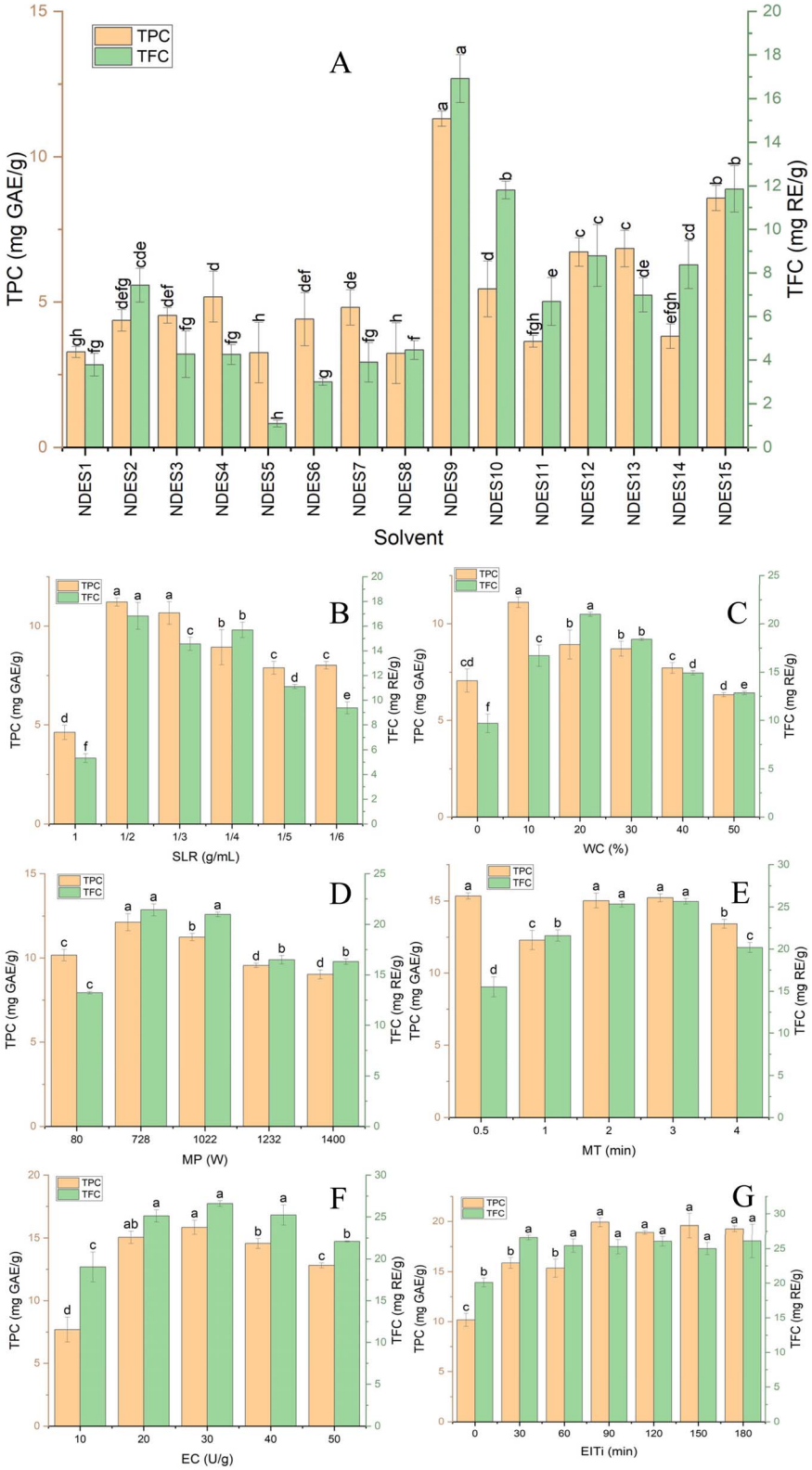

Fig. 2 MEAE conditions and their impact on TPC and TFC. Effect of NDESs on TPC and TFC (A). Effect of SLR (g mL^{-1}) on TPC and TFC (B). Effect of WC (%) on TPC and TFC (C). Effect of MP (W) on TPC and TFC (D). Effect of MT (min) on TPC and TFC (E). Effect of EC (U g^{-1}) on TPC and TFC (F). Effect of EIT (min) on TPC and TFC (G). The letters a, b…, and h represent statistically significant differences.

© 2026 The Author(s). Published by the Royal Society of Chemistry

Open Access Article. Published on 12 janvris 2026. Downloaded on 06.04.2026 16:18:23.
This article is licensed under a Creative Commons Attribution-NonCommercial 3.0 Unported Licence.

exceeded 20%, TPC and TFC yields declined. This trend aligns with research on *M. communis* leaves, which showed that the TPC yield was lower at 20% ethanol (80% water) and peaked at 40% ethanol (60% water). This illustrates that excessive water content increases the solvent polarity but reduces the solubility of target compounds, according to the "like dissolves like" principle.[16] When the WC in the NDES is excessive, the hydrogen bonds among NDES molecules are broken (Fig. S1). This phenomenon reduces the interaction between the NDES and phenolic compounds, thereby decreasing the effectiveness of the extraction process. Based on these observations, the effective water content for extracting TFC was 20%, while TPC showed the highest yield at 10% WC.

3.2.3 Impact of microwave power. The results of single-factor experiments for the extraction of phenolics and flavonoids from MP are shown in Fig. 2D. The experiments were performed using NDES9 with MP at 5 different levels: 280 W, 728 W, 1022 W, 1232 W, and 1400 W. When the MP increased from 280 W to 728 W, TPC and TFC rose significantly. Excessively high power can rapidly increase the solution temperature, leading to the degradation of heat-sensitive compounds, excessive solvent evaporation, and even damage to the raw materials.[34] However, since then, both TPC and TFC values have remained constant and then decreased significantly at higher power. The authors evaluated the effect of different MP levels on the antioxidant activity of phenolic compounds from Roselle (*Hibiscus sabdariffa* Linn). Due to the breakdown of heat-sensitive chemicals and a decrease in water content acting as the solvent, the results demonstrated that the total anthocyanin and vitamin C content rose from 100 W and peaked at 325 W (13.8591 mg/100 g) before declining at higher power levels.[35] Low power is insufficient to break down plant cell walls, making it difficult for compounds to be released. It also reduces cavitation effects and slows down diffusion. Therefore, 728 W is identified as the optimal MP level, achieving the highest extraction efficiency for both TPC and TFC from coriander.

3.2.4 Impact of microwave time. The results of single-factor experiments for phenolic and flavonoid extraction of MT are shown in Fig. 2E. The experiments were performed with microwave durations ranging from 30 seconds to 4 minutes. For TPC, a relatively high value is observed at 30 seconds, before reaching its peak at 3 minutes. Similarly, for TFC, the improvement in extraction efficiency is even more pronounced. Starting at 30 seconds, TFC increases significantly at 1 minute and reaches its highest value at 2 minutes. However, extending the microwave time to 3 minutes does not further enhance the yield and may even cause a decline in TFC. By 4 minutes, both TPC and TFC show a more evident reduction. In the experiment, the authors evaluated the effect of different microwave durations on extracting Rhein and Emodin compounds from *Rheum palmatum* L. The results showed that the extraction efficiency increased as the microwave time increased from 30 to 50 seconds. A duration of 50 seconds was selected, as more prolonged exposure (80 seconds) led to partial degradation of Rhein and Emodin.[36] A short microwave time may not be sufficient to disrupt the cell structure and release the target compounds. On the other hand, prolonged heat exposure from excessive microwave radiation may cause the oxidation of phenolic compounds.[37] Therefore, the time differs for each compound group: 3 minutes is the best condition for phenolic recovery, while 2 minutes is the most efficient condition to extract coriander's flavonoids.

3.2.5 Impact of enzyme concentration. The effect of EC on the extraction of phenolic and flavonoid compounds was evaluated, with the results presented in Fig. 2F. The MEAE process was investigated at enzyme concentrations ranging from 10 to 50 U g^{-1}. An increase in EC from 10 to 30 U g^{-1} resulted in approximately a twofold increase in TPC and a 1.3-fold increase in TFC. This enhancement is attributed to the greater formation of enzyme–substrate complexes, which facilitated more effective hydrolysis of cell wall components, thereby enhancing the release of phenolic and flavonoid compounds. However, a further increase to 50 U g^{-1} led to a decline in extraction efficiency, with TPC and TFC yields decreasing by 1.24- and 1.20-fold, respectively. Excessive enzyme concentrations may accelerate the hydrolysis of bound bioactive compounds into free forms, which, under elevated temperatures, become more mobile due to weakened hydrogen bonding within the solvent system. This increased mobility enhances their migration to the solvent interface, where exposure to oxidative and environmental stressors may promote degradation.[38] Similar findings were reported in studies involving *Acanthopanax senticosus*, where high enzyme concentrations adversely affected flavonoid recovery.[39] These results emphasize the importance of optimizing enzyme dosage to prevent compound degradation and ensure maximum extraction efficiency. Based on these observations, an enzyme concentration of 30 U g^{-1} was identified as optimal for efficiently extracting phenolics and flavonoids from DCP.

3.2.6 Impact of enzyme incubation time. The effect of EIT on the extraction of phenolic and flavonoid compounds by NDES9 was evaluated, with the results presented in Fig. 2G. Experiments were performed using varying incubation times (0–150 minutes). Without incubation (0 minutes), TPC and TFC exhibited the lowest yields, indicating limited extraction efficiency. This trend is likely due to the lack of interaction between the cellulase enzyme and the plant cell wall matrix, which prevents effective hydrolysis of cellulose chains and hinders the release of bound bioactive compounds. The rigid cellulose structure in DCP resists enzymatic breakdown, resulting in minimal release of compounds. Maximum extraction yields were achieved at 90 minutes for TPC (a 19.93% increase) and 30 minutes for TFC (a 26.60% increase), suggesting distinct extraction kinetics for phenolic and flavonoid compounds. The enzymatic degradation of cellulose enhances the porosity of the plant matrix by creating fissures and channels, thereby improving mass transfer and facilitating the release of target compounds.[38] However, prolonged incubation beyond these optimal times significantly reduced extraction efficiency by 18.93% for TPC and 26.51% for TFC. This decline is attributed to the degradation of thermolabile compounds under extended exposure to elevated temperatures, especially at the solvent interface, where oxidative and thermal stress can accelerate decomposition.[31] These findings are consistent with those reported by Vo *et al.* (2025), who observed a similar trend during

Open Access Article. Published on 12 janvris 2026. Downloaded on 06.04.2026 16:18:23.
This article is licensed under a Creative Commons Attribution-NonCommercial 3.0 Unported Licence.

the extraction of phenolics and flavonoids from *Elsholtzia ciliata*.[31] In conclusion, an EIT of 90 minutes for TPC and 30 minutes for TFC was selected as suitable for extracting phenolics and flavonoids.

The difference in retention durations between TFC and TPC was determined based on preliminary experiments. These trials revealed that flavonoid extraction reached equilibrium faster than phenolic extraction under similar experimental conditions. Therefore, a shorter retention time was selected for TFC to prevent unnecessary exposure and potential thermal degradation, while a longer duration was maintained for TPC to ensure complete recovery of phenolic compounds. Based on the experimental results investigating the effects of microwave and enzyme treatment duration, the appropriate time range was selected according to the recovery yields of phenolic and flavonoid compounds. The time point yielding the highest phenolic and flavonoid contents was designated as the center point, while the upper and lower boundaries were determined by the time points immediately preceding and following the center point, respectively. This approach enabled the selection of an optimal time range based on single-factor experiments. The investigation of time effects can also be considered a form of isothermal kinetic study.

3.3 Factor evaluation and optimization

3.3.1 Evaluating the significance of MEAE parameters. The Plackett–Burman design (PBD) model was employed to identify the key factors influencing TPC and TFC extraction yields, as presented in Tables S3 and S4. The coefficients exhibiting an absolute *t*-value greater than the critical threshold of 2.57 were deemed statistically significant, while those with |*t*-value| <2.57 were considered insignificant. These effects are quantitatively described by the regression equations presented in eqn (9) and (10). The model evaluated the effects of SLR (A), WC (B), MP (C), MT (D), EC (E), and EIT (F) on phenolic and flavonoid recovery from DCP. Regarding the ANOVA results in Table S5, the model demonstrated strong predictive performance, with a coefficient of determination (R^2) of 97.11% and an adjusted coefficient of determination (adj R^2) of 90.94% for TPC. For TFC, the coefficients of determination (R^2) of 95.88% and the adjusted (adj R^2) of 93.63% indicate its adequacy for accurately modeling the experimental data. As illustrated in Fig. 3A, EC (|*t*-value| = 6.73), MP (|*t*-value| = 6.44), and MT (|*t*-value| = 4.37) were significant positive contributors to TPC recovery. According to earlier research, MP had a major impact on TPC recovery from *Euphorbia hirta* leaves.[40] Meanwhile, Fig. 3B reveals that SLR (|*t*-value| = 11.99), WC (|*t*-value| = 3.40), and EIT (|*t*-value| = 2.68) significantly enhanced TFC extraction. Previous studies have indicated that WC plays a crucial role in modulating the efficiency of flavonoid extraction. In particular, investigations on Perilla leaves highlighted WC as a key determinant influencing (TFC) recovery, due to its effect on solvent polarity and dielectric behavior during MASE.[41] Based on these findings, EC, MP, and MT were selected for optimizing phenolic extraction, while SLR, WC, and EIT were identified as the critical variables influencing flavonoid yield.

$$y_{TPC} = 17.659 + 1.553x_3 + 1.055x_4 + 1.623x_5 \quad (9)$$

$$y_{TFC} = 17.608 + 6.553x_1 + 1.859x_2 - 1.465x_6 \quad (10)$$

3.3.2 Optimization of the MEAE process. In this study, fourteen experimental runs (Table S6) were conducted to investigate the synergistic effects of EC, MP, and MT on the extraction efficiency of TPC from DCP, while all other variables were maintained at their central levels. Similarly, another set of fourteen experiments (Table S7) was conducted to evaluate the combined effects of SLR, WC, and EIT on the extraction yield of TFC. The Box–Behnken design (BBD) was applied to analyze the individual and interactive effects of these process parameters on the performance of the MASE and EASE systems. Furthermore, three-dimensional response surface plots illustrated the interactive relationships between the independent variables and their corresponding responses. The regression models describing the correlations between the selected process variables and the responses – TPC and TFC – are presented in eqn (11) and (12), respectively:

$$y_{TPC} = 17.39 + 0.9562x_3 - 1.03x_4 + 1.59x_{34} - 2.04x_4^2 - 1.45x_5^2 \quad (11)$$

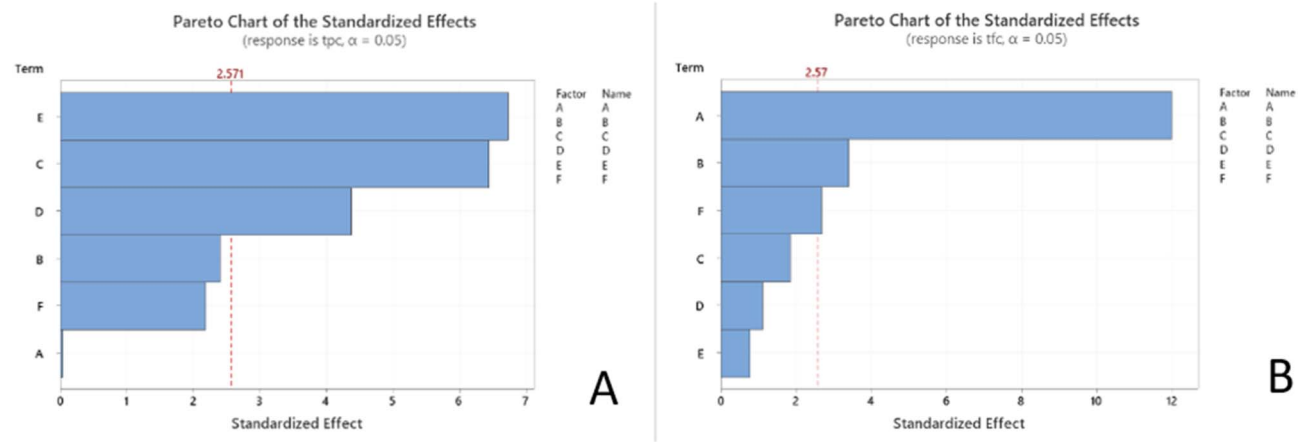

Fig. 3 The Plackett–Burman design's Pareto charts demonstrate how crucially extraction parameters affect the yield of the target compound: (A) TPC yield and (B) TFC yield. The variables analyzed included SRL (A), WC (B), MP (C), MT (D), EC (E), and EIT (F).

© 2026 The Author(s). Published by the Royal Society of Chemistry

Open Access Article. Published on 12 janvris 2026. Downloaded on 06.04.2026 16:18:23.
This article is licensed under a Creative Commons Attribution-NonCommercial 3.0 Unported Licence.

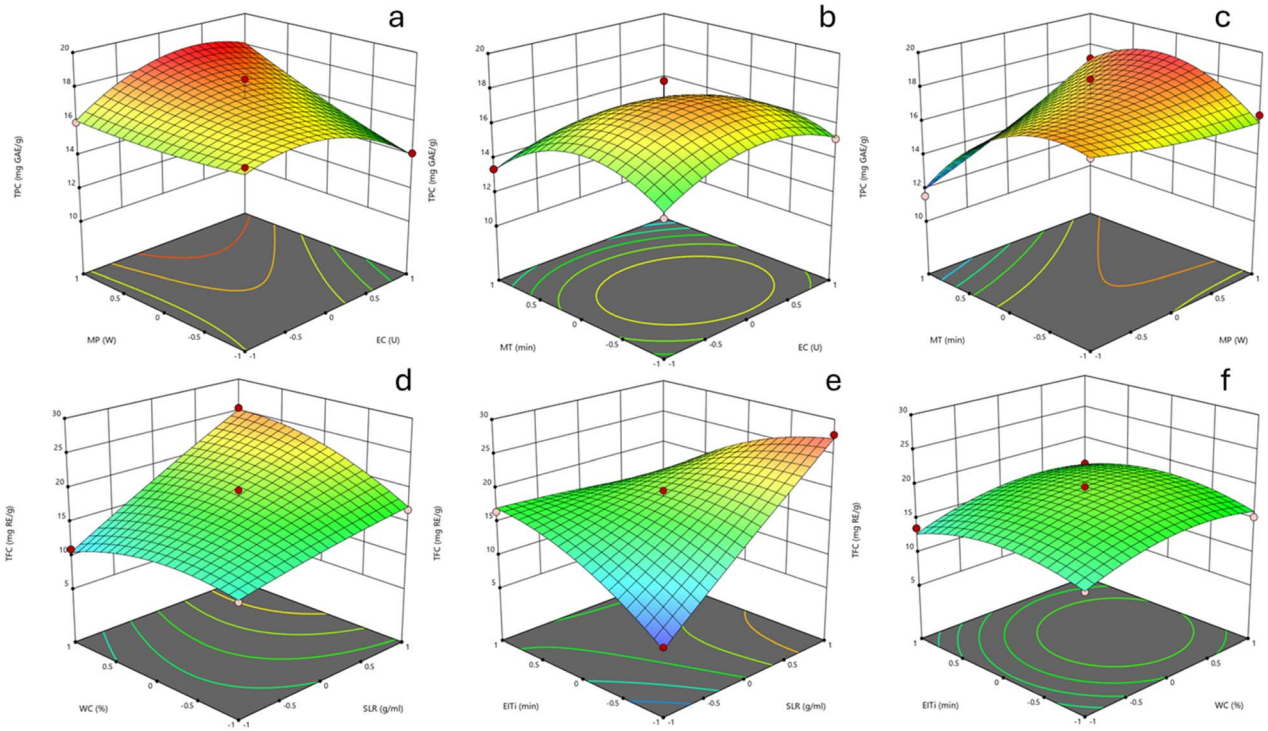

Fig. 4 3D response surface visualizations exhibiting the interactive impacts of MEAE conditions on TPC (a)–(c) and TFC (d)–(f).

$$y_{TFC} = 18.95 + 4.69x_1 + 1.30x_2 + 2.62x_{12} - 5.81x_{16} - 2.05{x_2}^2 - 2.23{x_6}^2 \quad (12)$$

The data were subjected to analysis of variance (ANOVA), and the results, as summarized in Table S8, indicate statistically significant p-values ($p < 0.05$) for both TPC and TFC, along with high adjusted R^2 values of 0.8032 for TPC and 0.9644 for TFC. These findings validate the adequacy of the second-order regression models, demonstrating their strong agreement with the experimental data and reliable predictive capability. The variables EC, MP, and MT, as well as their interactions, had a considerable impact on the extraction efficiency of phenolics. In contrast, the TFC yield was predominantly affected by SLR, WC, EIT, and their interactions.

Based on Fig. 4, the interactive effects of MEAE conditions on TPC and TFC are clearly observed. TPC gradually increases with the simultaneous increase in MP and EC, reaching a peak at higher levels of both factors. Notably, the combination of MT and MP significantly enhances TPC, highlighting the crucial roles of thermal energy and extraction duration in releasing phenolic compounds. For TFC, the interaction between WC and SLR indicates that both factors have a positive influence on TFC, particularly with increased SLR. Furthermore, a substantial increase in TFC is observed when both SLR and EIT are elevated, suggesting that extending enzymatic treatment time in a more diluted solvent system effectively promotes flavonoid release.

3.3.3 Model validation. Validation experiments were conducted under the optimal conditions for MEAE to evaluate the reliability of the developed regression models, as determined for each target compound. Using the Box–Behnken design (BBD), the optimal extraction parameters for maximizing TPC and TFC from DCP were established. For TPC, the optimal conditions included a SLR of 1/20 g mL^{-1}, a WC of 10% (w/w), a MP of 1022 W, a MT of 2.6 minutes, an EC of 40 U g^{-1}, an EIT of 90 minutes, and an EITem of 50 °C. In contrast, the optimal conditions for TFC are as follows: a SLR of 1/30 g mL^{-1}, WC: 23.7% (w/w), MP: 728 W, MT: 2 minutes, EC: 30 U g^{-1}, EIT: 30 minutes, and EITem: 50 °C. The results of the validation experiments, presented in Table S9, revealed prediction error rates of 2.51% for TPC and 5.80% for TFC, confirming the robustness and predictive accuracy of the regression models within the tested experimental range.

3.4 Second-order extraction kinetic models

To scale these processes for industrial applications, the EASE and MASE extraction kinetic modeling of TFC and TFC is crucial. While keeping the other parameters at ideal levels, kinetic experiments were carried out for the MASE process at different temperatures (30, 40, 50, 60, and 70 °C) and retention durations (20, 40, 60, 80, and 100 minutes for TPC and 10, 20, 30, 40, 50, and 60 minutes for TFC). The kinetic parameters, Arrhenius graphs, and second-order kinetic models of the phenolic and flavonoid extraction procedures are shown in Fig. 5 and Table S6. The viability of second-order kinetic models for recovering flavonoids and phenolics using EASE and MASE processes under varied conditions was demonstrated by the high values of determination coefficients ($R^2 \geq 0.9$). Due to the enhanced solvent diffusivity and solubility of bioactive compounds in the plant matrix, the h values rose as the temperature rose. Kenmogne Sidonie Béatrice *et al.* reported that the kinetics of the extraction process of total polyphenols from *Ximenia americana*

Open Access Article. Published on 12 janvris 2026. Downloaded on 06.04.2026 16:18:23.
This article is licensed under a Creative Commons Attribution-NonCommercial 3.0 Unported Licence.

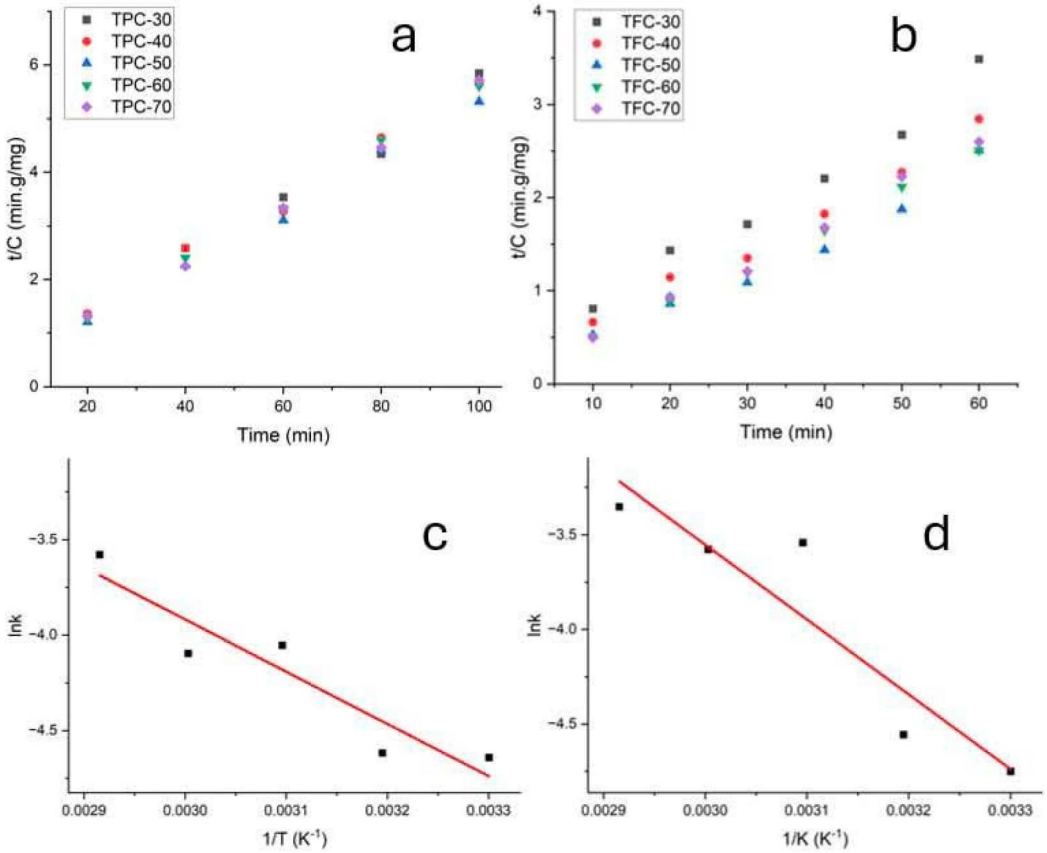

Fig. 5 Second-order kinetic plots of t/C_t *versus* time for (a) TPC and (b) TFC extraction; and Arrhenius plots of ln k *versus* $1/T$ for (c) TPC and (d) TFC extraction using the MEAE method.

roots using MASE showed that the pseudo-second-order kinetic model best described the process. The initial extraction rate (h) increased significantly with temperature, with the rate at 80 °C being nearly six times higher than that at 30 °C. The effective diffusion coefficient (D_{eff}) also demonstrated a temperature dependence, ranging from 2.215×10^{-13} to 7.232×10^{-13} m^2 s^{-1} within the temperature range of 303 K to 353 K, and increasing with temperature. When analyzed using the Arrhenius model, the data yielded an activation energy (E_a) of 14.436 kJ mol^{-1} with a high coefficient of determination ($R^2 = 0.859$), confirming a strong relationship between temperature and mass transfer rate during the extraction process.[42]

Arrhenius graphs ($1/T$ *vs.* ln k) established from second-order kinetic models were used to evaluate the activation energy for extracting phenolics and flavonoids from DPC using MASE and EASE procedures. The activation energy represents the minimum energy required to overcome the chemical barrier and extract flavonoids and phenolics. Because of the increased activation energy, more energy is required to solubilize flavonoids and phenolics.[43] Furthermore, the mechanism for extraction activities is determined by the activation energy. Solubilization is the extraction method if $E_a \geq 40$ kJ mol^{-1}. An activation energy of less than 20 kJ mol^{-1} indicates that diffusion is the dominant mechanism controlling the extraction. Diffusion and solubilization mechanisms are combined in the extraction process if E_a is between 20 and 40 kJ mol^{-1}.[42] TPC and TFC have been shown to have activation energy levels of 22.75 and 40.74 kJ mol^{-1}, respectively. While TFC is controlled by solubilization, TPC involves both diffusion and solubilization mechanisms. Given that flavonoids have a larger activation energy than phenolics, it is possible that flavonoid extraction will take place first, followed by phenolic extraction. Hobbi *et al.* used first-order and second-order kinetic models to study the extraction of polyphenols from apple pomace. Their findings indicated that the second-order model provided a better fit for predicting the influence of time and temperature on polyphenol recovery. Additionally, the study revealed that the extraction mechanism using 65% acetone, 50% ethanol, and water was primarily governed by diffusion (Table 2).[44]

3.5 Antioxidant activity

Fig. 6 presents the results indicating statistically significant variations among the different extraction methods regarding antioxidant activity and phytochemical content. Four extraction approaches were evaluated, including microwave-assisted extraction (MASE), enzyme-assisted extraction (EASE), conventional water extraction (CE), and combined microwave-enzymatic-assisted extraction (MEAE). Among these, the MEAE technique demonstrated substantial biological capacities for both TPC (18.15 ± 0.25 mg GAE g^{-1}) and TFC (26.36 ± 0.41 mg RE g^{-1}). Four assays were used to assess the extracts'

© 2026 The Author(s). Published by the Royal Society of Chemistry

Open Access Article. Published on 12 janvris 2026. Downloaded on 06.04.2026 16:18:23.
This article is licensed under a Creative Commons Attribution-NonCommercial 3.0 Unported Licence.

Table 2 Kinetic parameter of the extraction of phenolics and flavonoids from DCP

T (°C)	C_s (mg g^{-1})	h (mg min^{-1})	k (g mg^{-1} min^{-1})	a (g mg^{-1})	b (g min^{-1} mg^{-1})	R_1^2	E_a (kJ mol^{-1})	ln A_e	R_2^2
TPC									
30	18.59	3.33	0.01	0.05	0.30	0.9902	22.75	0.05	0.8805
40	18.62	3.42	0.01	0.05	0.29	0.9928			
50	19.31	6.48	0.02	0.05	0.15	0.9965			
60	18.38	5.62	0.02	0.05	0.18	0.9981			
70	18.14	9.19	0.03	0.06	0.11	0.9972			
TFC									
30	19.88	3.42	0.01	0.05	0.29	0.9815	40.74	80 097.51	0.8860
40	23.70	4.56	0.01	0.04	0.21	0.9864			
50	26.25	19.96	0.03	0.04	0.05	0.9706			
60	24.63	18.38	0.03	0.04	0.05	0.9965			
70	23.53	27.03	0.05	0.04	0.03	0.9933			

antioxidant capacity: DPPH, FRAP, ABTS, and hydroxyl radical (˙OH) scavenging. Due to the synergistic effect of the two extraction mechanisms, including physical and biological, MEAE consistently yields considerable results in four antioxidant assays (FRAP, ABTS, ˙OH, and DPPH), as presented in Fig. 6a and c. Under the optimized extraction conditions for TPC, the MEAE method exhibited an ABTS radical scavenging capacity of 30 ± 1 mg TAE g^{-1}, a FRAP activity of 9.8 ± 0.1 mg TAE g^{-1}, a DPPH radical inhibition of 0.7 ± 0.4 mg TAE g^{-1}, and a hydroxyl radical scavenging activity of 2.46 ± 0.05 mg TAE g^{-1}. Similarly, under the optimized TFC extraction conditions, MEAE achieved an ABTS of 28.5 ± 0.8 mg TAE g^{-1}, a FRAP of 6.0 ± 0.9 mg TAE g^{-1}, a DPPH of 0.61 ± 0.01 mg TAE g^{-1}, and a hydroxyl radical scavenging activity of 0.74 ± 0.02 mg TAE g^{-1}. This improvement is attributed to the combined action of enzymatic hydrolysis, which degrades phenolic–carbohydrate–flavonoid complexes, and microwave treatment, which promotes cell wall rupture and accelerates mass transfer. As a result of this process, phenolic and flavonoid chemicals are released in their free forms, which typically have more antioxidant activity than their bound counterparts. A similar study demonstrated that enzyme-assisted extraction from Vietnamese balm yields higher recovery of bioactive compounds, with superior DPPH, ABTS, and FRAP antioxidant activities compared to non-assisted extraction.[31] As a result, the order of antioxidant effectiveness among the extraction methods was MEAE > MASE > EASE > CE. The authors evaluated the MASE process combined with EASE for extracting compounds from *Punica granatum* peel and assessed their antioxidant activity. The study demonstrated that combining EASE and MASE resulted in a superior synergistic effect in recovering phenolic compounds from pomegranate peel, achieving maximum antioxidant activity. The phenolic content obtained using the combined method reached 305 mg GAE g^{-1}, which was significantly higher than that obtained using individual methods: conventional solvent extraction yielded only 94.6 mg GAE g^{-1}, EASE yielded 165.46 mg GAE g^{-1}, and MASE yielded 197.6 mg GAE g^{-1}.[45] Overall, the results highlight the efficiency of the combined microwave and enzyme-assisted extraction in enhancing the recovery of phenolic and flavonoid compounds, which possess potent antioxidant properties.

Given the established bioactivities of phenolic and flavonoid compounds, this research underscores their potential for large-scale extraction and industrial use. These compounds are commonly employed in processed foods to prevent lipid and protein oxidation, thereby extending shelf life and ensuring product stability. Beyond their antioxidant effects, they also exhibit notable antimicrobial properties, helping to control spoilage and pathogenic microorganisms. In broilers, dietary supplementation with polyphenols extracted from olive oil processing by-products enhanced meat antioxidant capacity.[46] The inclusion of gallic and linoleic acids improved lipid metabolism, productivity, and meat quality, as well as its antioxidant and antimicrobial properties.[46] Supplementation with oregano and laurel oils promoted growth performance and reduced lipid oxidation,[47] while rosemary extract in turkey diets effectively inhibited lipid oxidation and delayed meat spoilage.[46] Various snacks and beverages enriched with phenolics have recently been introduced, enhancing both sensory attributes and nutritional value. Additionally, extracts from *Coriandrum sativum* show great promise for use in dietary supplements, positioning them as a viable option for both the food and health sectors.[48] For example, coriander polyphenols have been reported to mitigate obesity and metabolic syndrome. Administration of coriander seeds to rats fed a high-cholesterol and high-triglyceride diet resulted in a hypolipidemic effect, accompanied by enhanced hepatic conversion of cholesterol to bile acids and increased fecal excretion.[49] In broiler chicks, dietary inclusion of whole coriander seeds significantly improved growth performance, body weight, feed intake, and feed conversion ratio.[46] In a human study conducted by Mexican researchers, volunteers received *C. sativum* seed powder, chia (*Salvia hispanica*) powder, or both for two months. Coriander supplementation increased antioxidant capacity and reduced glucose and cholesterol levels, while chia supplementation lowered cholesterol and triglycerides. The combined treatment further decreased glucose, cholesterol, and triglyceride levels, and all participants experienced weight loss.[50]

Open Access Article. Published on 12 janvris 2026. Downloaded on 06.04.2026 16:18:23.
This article is licensed under a Creative Commons Attribution-NonCommercial 3.0 Unported Licence.

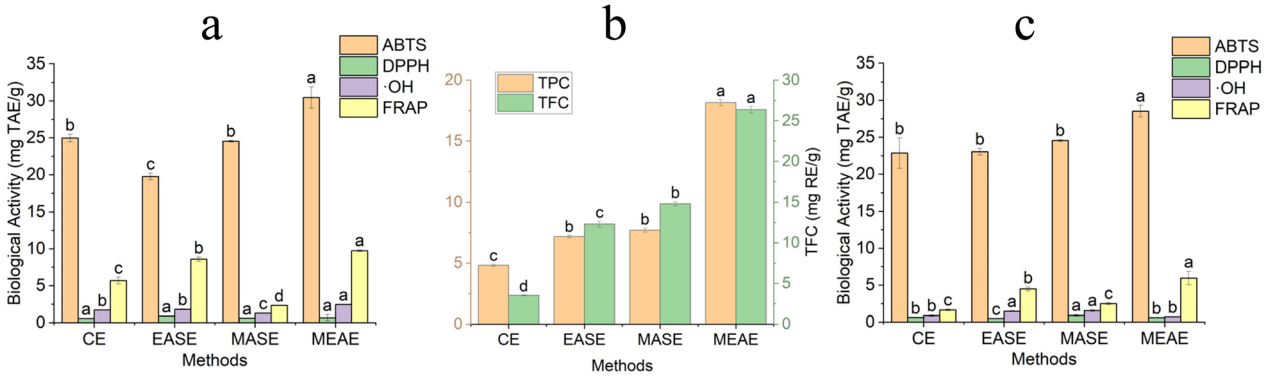

Fig. 6 Antioxidant activity and phytochemical content of extracts under optimal conditions. (a) Antioxidant activities of extracts from TPC optimized extraction conditions. (b) Phenolic and flavonoid contents in extracts from TPC and TFC optimized extractions. (c) Summary of the comparative antioxidant capacities (FRAP, DPPH, ABTS, and •OH) under optimized TFC conditions. The letters a, b, c, and d represent statistically significant differences.

3.6 Surface morphology and crystalline structure

SEM was used to determine the surface morphological changes of the DCP before and after treatment. Fig. 7A–E show the DCP's surfaces under different extraction conditions, revealing significant structural alterations depending on the technique used. The CE sample (Fig. 7B) shows a relatively intact, dense surface structure with minimal cell wall disruption. The tightly bound cellular matrices indicate limited cell rupture, which likely restricts the release of bioactive compounds, resulting in lower extraction efficiency. The EASE sample (Fig. 7C) exhibits disruption of the cellular structure. The surface appears uneven with small cracks, likely caused by the enzymatic hydrolysis of cell wall polysaccharides. This increases permeability and facilitates the release of phenolic compounds.[51] The MASE sample (Fig. 7D) reveals severe fragmentation and deep fissures across the surface, characterized by layered and broken structures. These morphological changes are attributed to localized microwave heating, which generates internal pressure and causes extensive cell rupture, thereby enhancing the extraction of intracellular components.[52] The MEAE sample (Fig. 7E) displays the most pronounced surface disruption, with prominent exfoliation and sponge-like cavities. The synergistic action of microwave and enzymatic treatment results in both cell wall weakening and thermal-induced rupture.

X-ray diffraction (XRD) is a powerful analytical technique widely used to assess changes in the crystalline structure of materials. It allows for the identification of crystalline phases and provides detailed structural information without compromising sample integrity. In this study, XRD was employed to evaluate the alterations in the crystallinity of DCP subjected to various extraction methods, including CE, EASE, MASE, and MEAE. The analysis primarily focused on determining the Crystallinity Index (CCI), a parameter indicative of structural reorganization influenced by the applied treatments. Diffractograms were collected over a θ range of 5.00° to 70.01°, with prominent peaks observed at approximately 18° and 22.5°, corresponding to the amorphous and crystalline regions, respectively (Fig. 7F). The untreated DCP exhibited a CCI of 12.27% ± 0.50%, while samples treated with CE, EASE, MASE, and MEAE displayed progressively higher CCI values of 15.81% ± 0.80%, 18.37% ± 0.60%, 21.76% ± 0.75%, and 26.81% ± 0.60%, respectively (Fig. 7G). These results suggest that the combined MEAE process, integrating both microwave energy and enzymatic hydrolysis, induces the most substantial enhancement in crystallinity, likely due to its ability to effectively disrupt amorphous cell wall components and promote the realignment of crystalline domains. An increase in crystallinity was observed after the various extraction treatments, indicating that removing amorphous components such as lignin and hemicellulose led to greater exposure of crystalline cellulose, thereby increasing the Crystallinity Index (CCI).[53] During the EASE process, the NDES facilitated the partial solubilization of amorphous structures through selective interactions while preserving the crystalline regions. In contrast, MASE raised the temperature of the solvent system, enhancing the solubility of both amorphous cellulose and hemicellulose. The combined MEAE process amplified these effects synergistically, resulting in more effective disruption of amorphous domains and substantial enrichment of crystalline cellulose.[54] Consequently, the MEAE-treated samples exhibited the highest CCI, confirming its superior capability in enhancing the material's crystalline structure.

3.7 The mechanism of natural deep eutectic solvent-based microwave-enzymatic-assisted extraction

A comprehensive extraction mechanism underlying the MEAE technique can be inferred from the kinetic data, SEM observations, and XRD analysis (Fig. 8). The microwave treatment induced localized heating and internal pressure, resulting in cell wall rupture and enhanced solvent penetration into plant tissues.[55] Concurrently, the enzymatic hydrolysis of polysaccharides weakened the cell wall matrix by breaking down cellulose and hemicellulose, facilitating mass transfer and compound release.[56] The NDES further contributed to this process by forming hydrogen bonds with cell wall components, partially dissolving amorphous lignin, and improving the solubility of phenolic and flavonoid compounds.[57] These synergistic effects collectively disrupted the plant structure, increased porosity, and exposed the crystalline cellulose regions observed in XRD patterns, resulting in a higher crystallinity

© 2026 The Author(s). Published by the Royal Society of Chemistry

Open Access Article. Published on 12 janvris 2026. Downloaded on 06.04.2026 16:18:23.
This article is licensed under a Creative Commons Attribution-NonCommercial 3.0 Unported Licence.

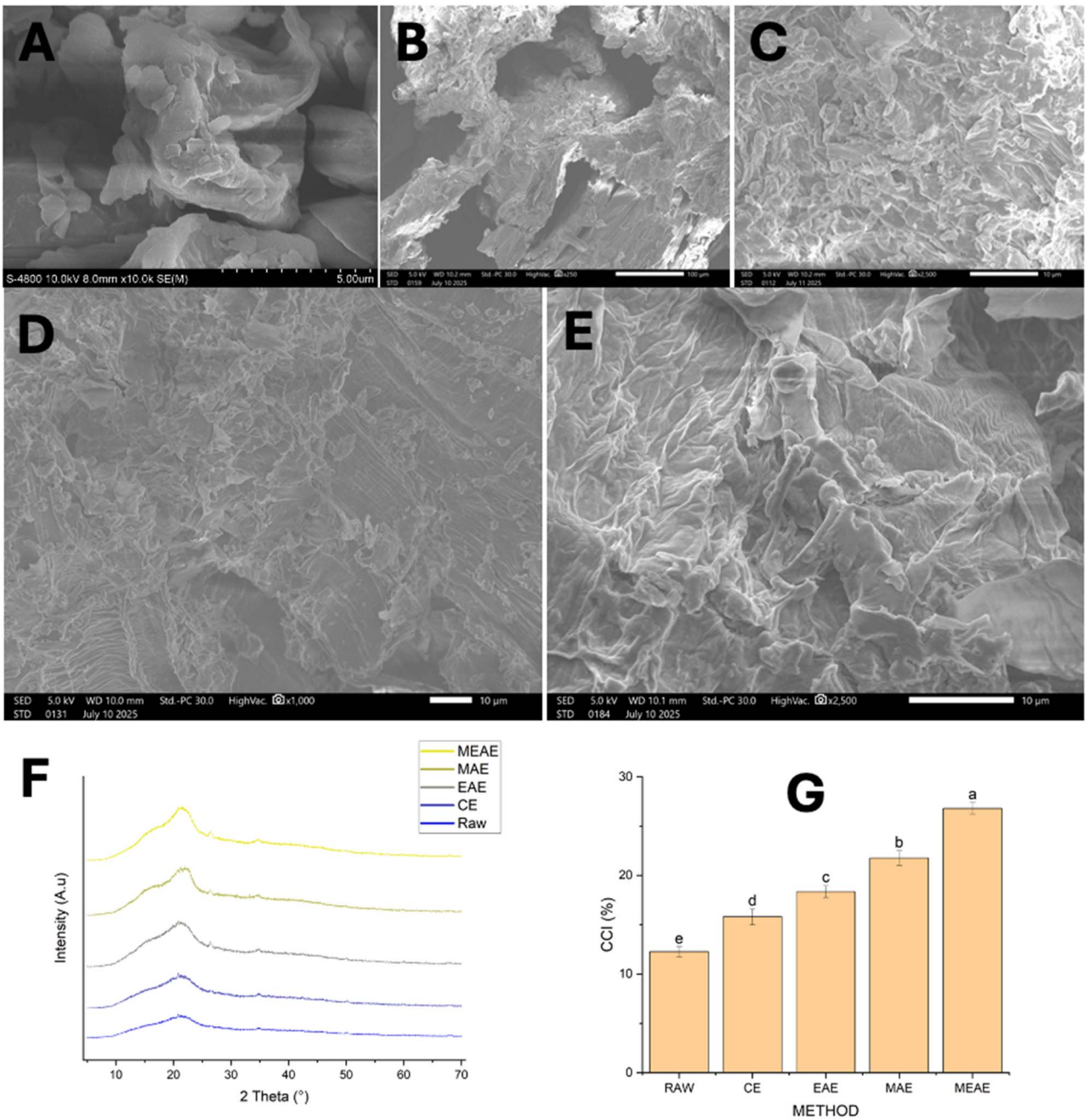

Fig. 7 Surface morphology and crystalline structure of DCP under different treatment conditions. (A) Surface morphology of untreated DCP; (B) surface morphology of DCP treated with CE; (C) surface morphology of DCP treated with NDES-based EASE; (D) surface morphology of DCP treated with NDES-based MASE; (E) surface morphology of DCP treated with NDES-based MEAE; crystalline structure analysis (F) and CCI profiles (G) of untreated and differently treated NDES-based DCP. The letters a, b, c, d, and e represent statistically significant differences.

index. The MEAE process effectively integrates physical and biochemical mechanisms, achieving efficient extraction while maintaining the structural stability of target bioactive compounds.

3.8 Reusability of solvent and cost and energy estimation

The reusability of NDES9 was evaluated through five consecutive extraction cycles (Fig. S2). For TPC, the first reuse retained 94.36 ± 2.90% of the initial extraction yield, which gradually declined to 85.65 ± 0.72%, 76.25 ± 0.97%, 74.29 ± 0.85%, and 68.90 ± 1.45% after the second to fifth cycles, respectively. Although a steady decrease was observed, more than 70% of the extraction efficiency was maintained after five cycles, demonstrating satisfactory solvent durability. A similar trend was observed for TFC, with retention rates of 91.67 ± 1.81%, 83.33 ± 1.62%, 82.63 ± 5.18%, 79.06 ± 0.71%, and 78.66 ± 0.52% for the first through fifth reuses, respectively. Statistical analysis (one-way ANOVA, $p < 0.05$) indicated that the differences between the first three cycles were insignificant, while significant decreases occurred from the fourth cycle onward. The

Open Access Article. Published on 12 janvris 2026. Downloaded on 06.04.2026 16:18:23.
This article is licensed under a Creative Commons Attribution-NonCommercial 3.0 Unported Licence.

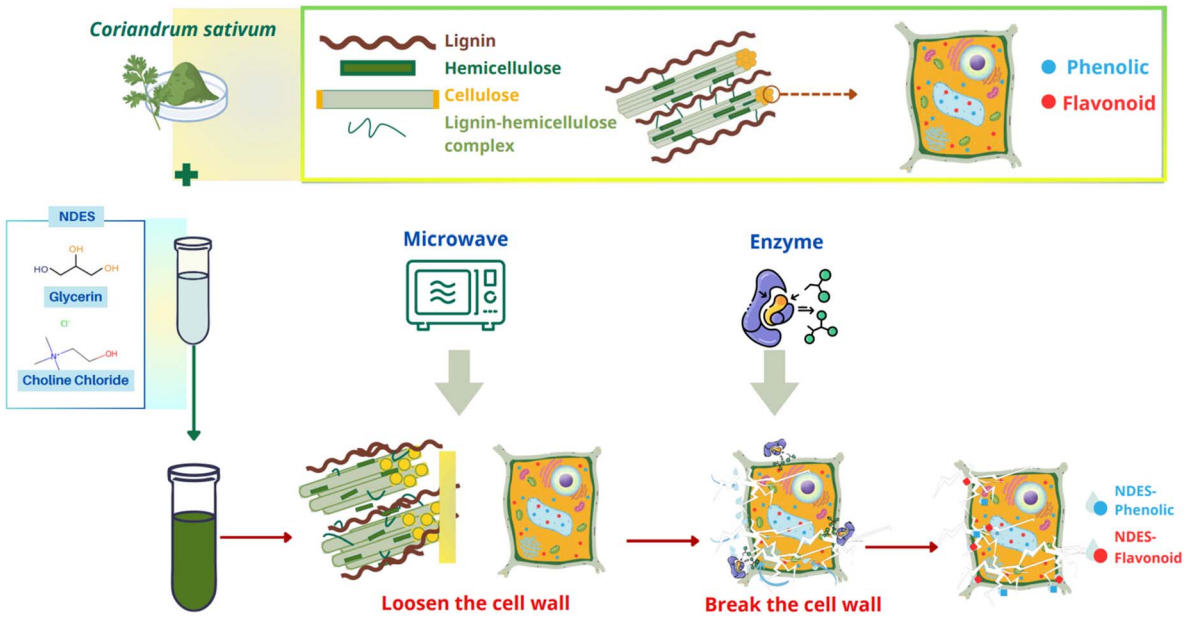

Fig. 8 The mechanism of the natural deep eutectic solvent-based microwave-enzymatic-assisted extraction process in recovering phenolics and flavonoids from *Coriandrum sativum* leaves.

gradual reduction in recovery efficiency may result from partial accumulation of residual plant pigments and polysaccharides in the solvent matrix, which can hinder mass transfer and reduce solvation efficiency. Nevertheless, TPC and TFC retained over 75–80% of their initial extraction efficiency after five reuse cycles without additional purification, confirming the solvent's strong structural stability. Thus, the NDES9-based MEAE process aligns with the principles of green chemistry, which can reduce the negative environmental impact of the extraction process.

The total cost and energy requirements for the optimized MEAE process were calculated for a 1 L batch, taking into account both material and energy consumption (Table S10). The estimated material cost for recovering phenolic and flavonoid compounds from 1 kg of DCP using NDES9 was USD 10.53 per kg, whereas recovery using water required USD 7.6 per kg. The estimated energy cost for recovering phenolic and flavonoid compounds from 1 kg DCP using NDES9 was 8.2 $USD, whereas recovery using water required 9.3 $USD. Although the operating cost for NDES9 extraction is higher than water extraction, the extraction efficiency of NDES9 is higher than water. Overall, the operating cost efficiency of NDES9 is better than that of water. Therefore, the NDES-based MEAE system has high potential for large-scale extraction of phenolic and flavonoid compounds from plants.

4 Conclusions

This study demonstrates that optimized MEAE conditions, based on statistical modeling, effectively enhance the recovery of antioxidants from *Coriandrum sativum* leaves. Among all tested NDESs, the glycerol-choline chloride system exhibited the highest extraction efficiency for both phenolic and flavonoid compounds. FTIR analysis confirmed the formation of hydrogen bonds between hydroxyl and carboxyl groups, verifying the solvent's structural stability and strong solvation ability. The optimal extraction conditions for TPC and TFC were generally similar, differing only in microwave extraction time and enzyme incubation time. The MT and EIT for TPC recovery are 2.6 and 90 minutes, whilst those of TFC recovery are 2 and 30 minutes. Kinetic modeling revealed that TPC extraction followed a combined diffusion-solubilization mechanism, whereas TFC extraction was primarily governed by solubilization. Improved extraction efficiency resulted from the synergy of microwave-assisted cell disruption and enzyme-catalyzed hydrolysis, as supported by SEM and XRD evidence of cell wall rupture and increased crystallinity. Additionally, the NDES system demonstrated high reusability, maintaining an extraction efficiency of approximately 75% after several cycles, highlighting its potential as a green, efficient, and sustainable solvent for industrial-scale applications. The findings highlight the potential of the extract as a natural preservative to replace synthetic additives that may pose health risks. Moreover, the extract can be further processed into concentrated paste, capsules, or dried powder for incorporation into various food products such as beverages and snack foods. It also shows promise as a partial fat replacer in processed foods like fish balls and sausages, contributing to extended shelf life and improved product quality.

Author contributions

Tan Phat Vo: conceptualization, methodology, software, formal analysis, investigation, data curation, writing – original draft, writing – review & editing, and visualization. Minh Thu Nguyen: investigation and formal analysis. Thuy Anh Nguyen: writing –

© 2026 The Author(s). Published by the Royal Society of Chemistry

Open Access Article. Published on 12 janvris 2026. Downloaded on 06.04.2026 16:18:23.
This article is licensed under a Creative Commons Attribution-NonCommercial 3.0 Unported Licence.

original draft and visualization. Gia Vinh Nguyen: investigation and formal analysis. Hoang Nhan Nguyen: writing – original draft. Gia Bao Pham: writing – original draft. Minh Hoa Ha: investigation and formal analysis. Dinh Quan Nguyen: writing – original draft, investigation, formal analysis, and supervision.

Conflicts of interest

The authors declare that they have no known competing financial interests or personal relationships that could have appeared to influence the work reported in this paper.

Abbreviations

DCP	Dried coriander powder
CE	Conventional extraction
MASE	Microwave-assisted extraction
EASE	Enzyme-assisted extraction
MEAE	Microwave-enzymatic-assisted extraction
TPC	Total phenolic content
TFC	Total flavonoid content
NDES	Natural deep eutectic solvents
SLR	Solid-to-liquid ratio
WC	Water content
MP	Microwave power
MT	Microwave time
EC	Enzyme concentration
EIT	Enzyme incubation time
EITem	Enzyme incubation temperature
CSE	Crude sample extract
ABTS	[2,2′-Azino-bis(3-ethylbenzothiazoline-6-sulfonic acid)]
DPPH	(2,2-Diphenyl-1-picrylhydrazyl)
FRAP	(Ferric reducing antioxidant power)
SEM	Scanning electron microscopy
XRD	X-ray diffraction
CCI	Cellulose crystallinity index

Data availability

Data will be made available on request.

Supplementary information (SI): detailed experimental data and statistical models supporting the primary findings of this study. Fig. S1: visual representation or data regarding the impact of excessive water content on the hydrogen bond network within the NDES. Fig. S2: performance data for the reusability of NDES9 across five consecutive extraction cycles. Table S1: details of the single-factor experimental design used for microwave-assisted and eyzyme-assisted extraction. Table S2: the standard metric for the Plackett–Burman Design (PBD) used to screen significant extraction variables. Tables S3 and S4: the estimated effects and coefficients for Total Phenolic Content (TPC) and Total Flavonoid Content (TFC) derived from the PBD model. Table S5: analysis of variance (ANOVA) results confirming the adequacy and predictive power of the PBD screening model. Tables S6 and S7: experimental runs and response values for the Box–Behnken Design (BBD) used in the optimization of TPC and TFC extraction. Table S8: ANOVA for the second-order regression models (BBD) validating the significance of linear, quadratic, and interaction terms. Table S9: results of validation experiments comparign experimental values with predicted yields to assess model robustness. Table S10: breakdown of the cost and energy estimation for the 1 L batch extraction process comparing NDES-based and water-based. See DOI: https://doi.org/10.1039/d5fb00536a.

Acknowledgements

We acknowledge the Ho Chi Minh City University of Technology (HCMUT), VNU-HCM for supporting this study.

References

1 B. Laribi, K. Kouki, M. M'Hamdi and T. Bettaieb, Coriander (*Coriandrum sativum* L.) and its bioactive constituents, *Fitoterapia*, 2015, **103**, 9–26, DOI: 10.1016/j.fitote.2015.03.012.
2 H. Wangensteen, A. B. Samuelsen and K. E. Malterud, Antioxidant activity in extracts from coriander, *Food Chem.*, 2004, **88**(2), 293–297, DOI: 10.1016/j.foodchem.2004.01.047.
3 I. Iqbal, P. Wilairatana, F. Saqib, B. Nasir, M. Wahid, M. F. Latif, A. Iqbal, R. Naz and M. S. Mubarak, Plant Polyphenols and Their Potential Benefits on Cardiovascular Health: A Review, *Molecules*, 2023, **28**(17), DOI: 10.3390/molecules28176403.
4 B. B. Hansen, S. Spittle, B. Chen, D. Poe, Y. Zhang, J. M. Klein, A. Horton, L. Adhikari, T. Zelovich, B. W. Doherty, *et al.*, Deep Eutectic Solvents: A Review of Fundamentals and Applications, *Chem. Rev.*, 2021, **121**(3), 1232–1285, DOI: 10.1021/acs.chemrev.0c00385.
5 O. R. Alara, N. H. Abdurahman and C. I. Ukaegbu, Extraction of phenolic compounds: a review, *Curr. Res. Food Sci.*, 2021, **4**, 200–214, DOI: 10.1016/j.crfs.2021.03.011.
6 C.-H. Chan, R. Yusoff, G. Ngoh and F. Kung, Extraction of Anti-diabetic Active Ingredient, Quercetin from Herbal Plant Using Microwave-assisted, *Extraction (MAE) Technique*, 2011, **KK-PO2-5**, DOI: 10.13140/2.1.3487.4885.
7 M. Chaliha, W. David, D. Edwards, S. Pun, H. Smyth and Y. Sultanbawa, Bioactive rich extracts from *Terminalia ferdinandiana* by enzyme-assisted extraction: a simple food safe extraction method, *J. Med. Plants Res.*, 2017, **11**, 96–106, DOI: 10.5897/JMPR2016.6285.
8 T. P. Vo, T. H. P. Nguyen, V. K. Nguyen, T. C. T. Dang, L. G. K. Nguyen, T. Q. Chung, T. T. H. Vo and D. Q. Nguyen, Extracting bioactive compounds and proteins from *Bacopa monnieri* using natural deep eutectic solvents, *PLoS One*, 2024, **19**(3), e0300969, DOI: 10.1371/journal.pone.0300969.
9 Y. C. Sakurai, I. V. Pires, N. R. Ferreira, S. G. Moreira, L. H. Silva and A. M. Rodrigues, Preparation and Characterization of Natural Deep Eutectic Solvents (NADESs): Application in the Extraction of Phenolic Compounds from Araza Pulp (*Eugenia stipitata*), *Foods*, 2024, **13**(13), DOI: 10.3390/foods13131983.

Open Access Article. Published on 12 janvris 2026. Downloaded on 06.04.2026 16:18:23.
This article is licensed under a Creative Commons Attribution-NonCommercial 3.0 Unported Licence.

10 L. Wu, L. Li, S. Chen, L. Wang and X. Lin, Deep eutectic solvent-based ultrasonic-assisted extraction of phenolic compounds from *Moringa oleifera* L. leaves: optimization, comparison and antioxidant activity, *Sep. Purif. Technol.*, 2020, **247**, 117014, DOI: 10.1016/j.seppur.2020.117014.
11 A. M. Shraim, T. A. Ahmed, M. M. Rahman and Y. M. Hijji, Determination of total flavonoid content by aluminum chloride assay: a critical evaluation, *LWT–Food Sci. Technol.*, 2021, **150**, 111932, DOI: 10.1016/j.lwt.2021.111932.
12 L. M. S. Pereira, T. M. Milan and D. R. Tapia-Blácido, Using response surface methodology (RSM) to optimize 2G bioethanol production: a review, *Biomass Bioenergy*, 2021, **151**, 106166, DOI: 10.1016/j.biombioe.2021.106166.
13 Y. S. Ho and G. McKay, Pseudo-second order model for sorption processes, *Process Biochem.*, 1999, **34**(5), 451–465, DOI: 10.1016/S0032-9592(98)00112-5.
14 H. Ran, X. Zhang, J. Long, Z. Wang, S. Zhuang, X. Zhang, Y. Jiang, J. Zhang and G. Wang, Ultrasound-assisted extraction of naringin from Exocarpium Citri Grandis using a novel ternary natural deep eutectic solvent based on glycerol: process optimization using ANN-GA, extraction mechanism and biological activity, *Ultrason. Sonochem.*, 2025, **121**, 107551, DOI: 10.1016/j.ultsonch.2025.107551.
15 X. Zhang, J. Su, X. Chu and X. Wang, A Green Method of Extracting and Recovering Flavonoids from Acanthopanax senticosus Using Deep Eutectic Solvents, *Molecules*, 2022, **27**(3), DOI: 10.3390/molecules27030923.
16 F. Dahmoune, B. Nayak, K. Moussi, H. Remini and K. Madani, Optimization of microwave-assisted extraction of polyphenols from Myrtus communis L. leaves, *Food Chem.*, 2015, **166**, 585–595, DOI: 10.1016/j.foodchem.2014.06.066.
17 P. Rodsamran and R. Sothornvit, Extraction of phenolic compounds from lime peel waste using ultrasonic-assisted and microwave-assisted extractions, *Food Biosci.*, 2019, **28**, 66–73, DOI: 10.1016/j.fbio.2019.01.017.
18 D. Mukhopadhyay, P. Dasgupta, D. Sinha Roy, S. Palchoudhuri, I. Chatterjee, S. Ali and S. Ghosh Dastidar, A Sensitive *In vitro* Spectrophotometric Hydrogen Peroxide Scavenging Assay using 1,10-Phenanthroline, *Free Radicals Antioxid.*, 2015, **6**(1), 124–132, DOI: 10.5530/fra.2016.1.15.
19 H. T. Vu, C. J. Scarlett and Q. V. Vuong, Maximising recovery of phenolic compounds and antioxidant properties from banana peel using microwave assisted extraction and water, *J. Food Sci. Technol.*, 2019, **56**(3), 1360–1370, DOI: 10.1007/s13197-019-03610-2.
20 U. P. Agarwal, S. A. Ralph, C. Baez, R. S. Reiner and S. P. Verrill, Effect of sample moisture content on XRD-estimated cellulose crystallinity index and crystallite size, *Cellulose*, 2017, **24**(5), 1971–1984, DOI: 10.1007/s10570-017-1259-0.
21 I. V. Pires, Y. C. Sakurai, N. R. Ferreira, S. G. Moreira, A. M. da Cruz Rodrigues and L. H. da Silva, Elaboration and Characterization of Natural Deep Eutectic Solvents (NADESs): Application in the Extraction of Phenolic Compounds from pitaya, *Molecules*, 2022, **27**(23), DOI: 10.3390/molecules27238310.
22 O. Zannou and I. Koca, Greener extraction of anthocyanins and antioxidant activity from blackberry (Rubus spp) using natural deep eutectic solvents, *LWT–Food Sci. Technol.*, 2022, **158**, 113184, DOI: 10.1016/j.lwt.2022.113184.
23 K. Subashini and S. Periandy, Spectroscopic (FT-IR, FT-Raman, UV, NMR, NLO) investigation and molecular docking study of 1-(4-Methylbenzyl) piperazine, *J. Mol. Struct.*, 2017, **1134**, 157–170, DOI: 10.1016/j.molstruc.2016.12.048.
24 Z. Li, C. Cheng, L. Zhang, J. Xue, Q. Sun, H. Wang, R. Cui, R. Liu and L. Song, Extraction of pigments from chestnut (*Castanea mollissima*) shells using green deep eutectic solvents: optimization, HPLC-MS identification, stability, and antioxidant activities, *Food Chem.*, 2025, **488**, 144916, DOI: 10.1016/j.foodchem.2025.144916.
25 M. Abdollahzadeh, M. Khosravi, B. Hajipour Khire Masjidi, A. Samimi Behbahan, A. Bagherzadeh, A. Shahkar and F. Tat Shahdost, Estimating the density of deep eutectic solvents applying supervised machine learning techniques, *Sci. Rep.*, 2022, **12**(1), 4954, DOI: 10.1038/s41598-022-08842-5.
26 D. Troter, M. Zlatkovic, D. Đokić-Stojanović and S. Konstantinović, Citric acid-based deep eutectic solvents: physical properties and their use as cosolvents in sulphuric acid-catalysed ethanolysis of oleic acid, *Adv. Technol.*, 2016, **5**, 53–65, DOI: 10.5937/savteh1601053T.
27 M. B. Taysun, E. Sert and F. S. Atalay, Effect of Hydrogen Bond Donor on the Physical Properties of Benzyltriethylammonium Chloride Based Deep Eutectic Solvents and Their Usage in 2-Ethyl-Hexyl Acetate Synthesis as a Catalyst, *J. Chem. Eng. Data*, 2017, **62**(4), 1173–1181, DOI: 10.1021/acs.jced.6b00486.
28 O. A. O. Alshammari, G. A. A. Almulgabsagher, K. S. Ryder and A. P. Abbott, Effect of solute polarity on extraction efficiency using deep eutectic solvents, *Green Chem.*, 2021, **23**(14), 5097–5105, DOI: 10.1039/d1gc01747k.
29 Glycerol, *National Library of Medicince*, https://pubchem.ncbi.nlm.nih.gov/compound/753, accessed 2025 October 31.
30 J. K. U. Ling, Y. S. Chan and J. Nandong, Degradation kinetics modeling of antioxidant compounds from the wastes of Mangifera pajang fruit in aqueous and choline chloride/ascorbic acid natural deep eutectic solvent, *J. Food Eng.*, 2021, **294**, 110401, DOI: 10.1016/j.jfoodeng.2020.110401.
31 T. P. Vo, T. H. Trang Nguyen, H. B. Tran Nguyen, H. N. Nguyen, N. V. Nhi Le, M. H. Ha, G. B. Pham and D. Q. Nguyen, Enhancing phenolic and flavonoid recovery from Vietnamese balm using green solvent-based ultrasonic-enzymatic-assisted extraction, *Ultrason. Sonochem.*, 2025, **121**, 107546, DOI: 10.1016/j.ultsonch.2025.107546.
32 R. Rashid, S. Mohd Wani, S. Manzoor, F. A. Masoodi and M. Masarat Dar, Green extraction of bioactive compounds from apple pomace by ultrasound assisted natural deep

 © 2026 The Author(s). Published by the Royal Society of Chemistry

Open Access Article. Published on 12 janvris 2026. Downloaded on 06.04.2026 16:18:23.
This article is licensed under a Creative Commons Attribution-NonCommercial 3.0 Unported Licence.

eutectic solvent extraction: optimisation, comparison and bioactivity, *Food Chem.*, 2023, **398**, 133871, DOI: 10.1016/j.foodchem.2022.133871.

33 B. Kaufmann and P. Christen, Recent extraction techniques for natural products: microwave-assisted extraction and pressurised solvent extraction, *Phytochem. Anal.*, 2002, **13**(2), 105–113, DOI: 10.1002/pca.631.

34 M. Zhao, Y. Li, X. Xu, J. Wu, X. Liao and F. Chen, Degradation Kinetics of Malvidin-3-glucoside and Malvidin-3,5-diglucoside Exposed to Microwave Treatment, *J. Agric. Food Chem.*, 2013, **61**(2), 373–378, DOI: 10.1021/jf304410t.

35 I. S. M. Purbowati and A. Maksum, The antioxidant activity of Roselle (Hibiscus sabdariffa Linii) phenolic compounds in different variations microwave-assisted extraction time and power, *IOP Conf. Ser.: Earth Environ. Sci.*, 2019, **406**(1), 012005, DOI: 10.1088/1755-1315/406/1/012005.

36 Y. Fan, Z. Niu, C. Xu, L. Yang and T. Yang, Protic Ionic Liquids as Efficient Solvents in Microwave-Assisted Extraction of Rhein and Emodin from Rheum palmatum L, *Molecules*, 2019, **24**(15), DOI: 10.3390/molecules24152770.

37 I. T. Tomasi, S. C. R. Santos, R. A. R. Boaventura and C. M. S. Botelho, Optimization of microwave-assisted extraction of phenolic compounds from chestnut processing waste using response surface methodology, *J. Cleaner Prod.*, 2023, **395**, 136452, DOI: 10.1016/j.jclepro.2023.136452.

38 H. Cao, O. Saroglu, A. Karadag, Z. Diaconeasa, G. Zoccatelli, C. A. Conte-Junior, G. A. Gonzalez-Aguilar, J. Ou, W. Bai, C. M. Zamarioli, *et al.*, Available technologies on improving the stability of polyphenols in food processing, *Food Front.*, 2021, **2**(2), 109–139, DOI: 10.1002/fft2.65.

39 M. Bener, F. B. Şen, A. N. Önem, B. Bekdeşer, S. E. Çelik, M. Lalikoglu, Y. S. Aşçı, E. Capanoglu and R. Apak, Microwave-assisted extraction of antioxidant compounds from by-products of Turkish hazelnut (*Corylus avellana* L.) using natural deep eutectic solvents: modeling, optimization and phenolic characterization, *Food Chem.*, 2022, **385**, 132633, DOI: 10.1016/j.foodchem.2022.132633.

40 O. A. Olalere and C.-Y. Gan, Intensification of microwave energy parameters and main effect analysis of total phenolics recovery from Euphorbia hirta leaf, *J. Food Meas. Charact.*, 2020, **14**(2), 886–893, DOI: 10.1007/s11694-019-00338-7.

41 T. P. Vo, M. T. Nguyen, T. A. T. Ho, N. L. U. Luong, L. M. U. Van, L. T. T. Nguyen and D. Q. Nguyen, Combining the natural deep eutectic solvents and high-speed-shearing-enzymatic-assisted extraction to recover flavonoids and terpenoids from perilla leaves, *J. Mol. Liq.*, 2024, **411**, 125720, DOI: 10.1016/j.molliq.2024.125720.

42 T. P. Vo, H. N. Nguyen, G. B. Pham, N. A. T. La, X. D. A. Pham and D. Q. Nguyen, Application of ultrasound-microwave-assisted extraction to extract phenolic and terpenoid compounds from celery stalk, *J. Agric. Food Res.*, 2025, **24**, 102362, DOI: 10.1016/j.jafr.2025.102362.

43 J. Ampofo, M. Ngadi and H. S. Ramaswamy, Elicitation kinetics of phenolics in common bean (*Phaseolus vulgaris*) sprouts by thermal treatments, *Legume Sci.*, 2020, **2**(4), e56, DOI: 10.1002/leg3.56.

44 P. Hobbi, O. V. Okoro, C. Delporte, H. Alimoradi, D. Podstawczyk, L. Nie, K. V. Bernaerts and A. Shavandi, Kinetic modelling of the solid–liquid extraction process of polyphenolic compounds from apple pomace: influence of solvent composition and temperature, *Bioresour. Bioprocess.*, 2021, **8**(1), 114, DOI: 10.1186/s40643-021-00465-4.

45 M. Kumar, M. Tomar, S. Punia, R. Amarowicz and C. Kaur, Evaluation of Cellulolytic Enzyme-Assisted Microwave Extraction of Punica granatum Peel Phenolics and Antioxidant Activity, *Plant Foods Hum. Nutr.*, 2020, **75**(4), 614–620, DOI: 10.1007/s11130-020-00859-3.

46 R. Branciari, R. Galarini, D. Giusepponi, M. Trabalza-Marinucci, C. Forte, R. Roila, D. Miraglia, M. Servili, G. Acuti and A. Valiani, Oxidative Status and Presence of Bioactive Compounds in Meat from Chickens Fed Polyphenols Extracted from Olive Oil Industry Waste, *Sustainability*, 2017, **9**(9), DOI: 10.3390/su9091566.

47 I. Giannenas, A. Tzora, I. Sarakatsianos, A. Karamoutsios, S. Skoufos, N. Papaioannou, I. Anastasiou and I. Skoufos, The Effectiveness of the Use of Oregano and Laurel Essential Oils in Chicken Feeding, *Ann. Anim. Sci.*, 2016, **16**(3), 779–796, DOI: 10.1515/aoas-2015-0099.

48 S. Scandar, C. Zadra and M. C. Marcotullio, Coriander (*Coriandrum sativum*) Polyphenols and Their Nutraceutical Value against Obesity and Metabolic Syndrome, *Molecules*, 2023, **28**(10), DOI: 10.3390/molecules28104187.

49 A. K. Biswas, C. K. Beura, A. S. Yadav, N. K. Pandey, S. K. Mendiratta and J. M. Kataria, Influence of novel bioactive compounds from selected fruit by-products and plant materials on the quality and storability of microwave-assisted cooked poultry meat wafer during ambient temperature storage, *LWT–Food Sci. Technol.*, 2015, **62**(2), 727–733, DOI: 10.1016/j.lwt.2014.09.024.

50 A. I. Andrés, M. J. Petrón, J. D. Adámez, M. López and M. L. Timón, Food by-products as potential antioxidant and antimicrobial additives in chill stored raw lamb patties, *Meat Sci.*, 2017, **129**, 62–70, DOI: 10.1016/j.meatsci.2017.02.013.

51 D. Kammerer, A. Claus, A. Schieber and R. Carle, A Novel Process for the Recovery of Polyphenols from Grape (*Vitis vinifera* L.) Pomace, *J. Food Sci.*, 2005, **70**(2), C157–C163, DOI: 10.1111/j.1365-2621.2005.tb07077.x.

52 H. Baltacıoğlu, C. Baltacıoğlu, I. Okur, A. Tanrıvermiş and M. Yalıç, Optimization of microwave-assisted extraction of phenolic compounds from tomato: characterization by FTIR and HPLC and comparison with conventional solvent extraction, *Vib. Spectrosc.*, 2021, **113**, 103204, DOI: 10.1016/j.vibspec.2020.103204.

53 L. Zhu, K. Liang, M. Wang, T. Xing, C. Chen and Q. Wang, Microwave-assisted formic acid/cold caustic extraction for separation of cellulose and hemicellulose from biomass, *BioResources*, 2023, **18**, 6896–6912, DOI: 10.15376/biores.18.4.6896-6912.

Open Access Article. Published on 12 janvris 2026. Downloaded on 06.04.2026 16:18:23.
This article is licensed under a Creative Commons Attribution-NonCommercial 3.0 Unported Licence.

54 S. Vinhas, M. Sarraguça, T. Moniz, S. Reis and M. Rangel, A New Microwave-Assisted Protocol for Cellulose Extraction from Eucalyptus and Pine Tree Wood Waste, *Polymers*, 2024, **16**(1), DOI: 10.3390/polym16010020.
55 Comparative Analysis of Microwave-Assisted Extraction (MAE) and Traditional Extraction Techniques for Phytochemicals from Plants, *Int. J. Environ. Sci.*, 2025, 3390–3404, DOI: 10.64252/r5hzc522, acccessed 2025/11/04.
56 X. Wang, Y. Su, J. Su, J. Xue, R. Zhang, X. Li, Y. Li, Y. Ding and X. Chu, Optimization of Enzyme-Assisted Aqueous Extraction of Polysaccharide from Acanthopanax senticosus and Comparison of Physicochemical Properties and Bioactivities of Polysaccharides with Different Molecular Weights, *Molecules*, 2023, **28**(18), DOI: 10.3390/molecules28186585.
57 K. Antoun, M. Tabib, S. J. Salameh, M. Koubaa, I. Ziegler-Devin, N. Brosse and A. Khelfa, Isolation and Structural Characterization of Natural Deep Eutectic Solvent Lignin from Brewer's Spent Grains, *Polymers*, 2024, **16**(19), DOI: 10.3390/polym16192791.

© 2026 The Author(s). Published by the Royal Society of Chemistry